Effects of Relative Volatility Ranking to the Design of Reactive Distillation

Shih-Tse Tung and Cheng-Ching Yu
Dept. of Chemical Engineering, National Taiwan University, Taipei 106-17, Taiwan

DOI 10.1002/aic.11168
Published online March 30, 2007 in Wiley InterScience (www.interscience.wiley.com).

This work is aimed to provide a systematic design procedure to determine the process configuration, the relative position of the reactive zone, and separation sections. Instead of investigating real chemical systems, ideal chemical reaction systems with different relative volatility rankings will be studied. This provides a gradual transition as the reaction and separation properties change. The reaction considered is a reversible reaction, $A + B \Leftrightarrow C + D$, and this constitutes a quaternary system with 24 (4!) possible relative volatility arrangements. These 24 systems can further be grouped into six categories according to the ranking of relative volatilities of reactants and products. The likely process configurations will be explored and design will be optimized based on the total annual cost (TAC). The results clearly indicate that the relative volatility rankings play a dominant role in the reactive distillation configuration and the TAC varies by a factor of ~7 as we move from the most favorable case (reactants are intermediate keys) to the least favorable relative volatility ranking (products are intermediate keys). Finally, heuristics are given to correlate the relative volatility ranking to the TAC. *AIChE J,* 53: 1278–1297, 2007
Keywords: reactive distillation, process configuration, relative volatility, conceptual design

Introduction

The reactive distillation (RD) offers significant economic advantages in some systems, especially when reactions are reversible and/or when azeotropes are presented. More than 60 potential applications of RD in the chemical and petroleum industries have been well documented.[1–3] The literature up to 1992 was reviewed by Doherty and Buzad[4] and simulation and design (both software and hardware) aspects have been reviewed by Taylor and Krishna.[5] Recent books[1,2] present updated summaries. Despite recent progress in RD, generation of process alternatives and conceptual design (i.e., generating process configuration for placing reactive zone, rectifying section, and stripping section) is still lacking. This is clearly stated by Doherty and Malone[1]: "At the moment, there are relative few general methods available for generating all feasible alternatives, but some systematic studies are published. This is a very hard problem to solve and it is reasonable to expect that methods will be slower in coming." Part of the reason comes from the fact that most of the work focuses on real chemical systems, and each system has its own set of complexities in vapor–liquid equilibrium (VLE; e.g., azeotropes) and reaction kinetics (activity-based). The discrete nature of chemical species and specific applications seem to cloud the picture in understanding RD systems. On the other hand, the ideal RD[6] offers a continuous spectrum in studying the process behavior by stripping away all the nonideal VLE and specific reaction rates. Only a limited number of papers study the ideal RD systems and most of them focus on feasibility analysis.[7–9] Design of RD has been explored[10,11] and comparison to conventional multiunit reactor/column/recycle systems has been made.[12,13] The systems studied are the "neat" design where exact stoichiometric feeds are introduced to the system. For systems with unfavorable reaction kinetics (e.g., small chemical equilibrium constant) and VLE, the design with one excess reactant may be a viable choice.[14] Lee et al.[15] address the conceptual design

Correspondence concerning this article should be addressed to C.-C. Yu at ccyu@ntu.edu.tw.

Table 1. Physical Properties for the Process Studied

Activation energy (cal/mol)	Forward (E_F)			12,000	
	Backward (E_B)			17,000	
Specific reaction rate	Forward (k_F)			0.008	
at 366 K (kmol s^{-1} $kmol^{-1}$)	Backward (k_B)			0.004	
Heat of reaction (cal/mol)	λ			−5000	
Heat of vaporization (cal/mol)	ΔH_v			6944	
Relative volatilities (LLK/LK/HK/HHK)	$\alpha_{LLK} > \alpha_{LK} > \alpha_{HK} > \alpha_{HHK}$			8/4/2/1	
		LLK	LK	HK	HHK
Vapor pressure constants[a] $\ln P_i^S = A_{VP,i} - B_{VP,i}/T$	A_{VP}	13.04	12.34	11.45	10.96
	B_{VP}	3862	3862	3862	3862

issue based on feasibility analysis. The effects of physical properties, relative volatility, chemical equilibrium constant activation energies, preexponential factors, on the design of RD have been studied.[13,16] On the process level, the effects of the number of separation trays, number of reactive trays, column pressure, feed locations, and catalyst loading are also carefully examined.[13,16,17]

It is interesting to note that most of the ideal RD systems in the literature assuming that the reactants are the intermediate keys while the two products belong to heavy key and light key, respectively, for the quaternary system with A + B ⇔ C + D. Obviously, this is not the case in practice, not even for the methyl acetate example.[18] The boiling point ranking (for the reactants and products) plays an important role in conceptual design as shown in the acetic acid esterification example.[19,20] As the alcohol (for esterification) varies from C1 to C5, the process configuration changes as a result of variation in the ranking of pure components and azeotropes. Chin et al.[21] explore the configurations of batch RD for ternary systems, as physical properties of reactants and products change. Potential conflict between reaction and separation for reactive separations is also illustrated qualitatively.[22] In this work, we will explore the effects of the relative volatility ranking to the conceptual design of RD. In particular, how the relative position of reactive zone and separation sections varies as the boiling points of the reactants and products change. RD systems with ideal VLE are studied here with "neat" design (no excess in either reactant) and the reaction of interest is an exothermic second-order reaction, A + B ⇔ C + D. The remainder of this paper is organized as follows. First, classification and simulation are described. In the next section, the design procedure is given first, followed by flowsheet generation for all six process types. Results are discussed and heuristics are given followed by the conclusion.

Process and classification

Process. Let us use quaternary ideal RD systems to illustrate the effects of boiling point ranking on conceptual design. Consider the following second-order liquid phase reversible reaction:

$$A + B \Leftrightarrow C + D \tag{1}$$

The forward and backward specific rates following the Arrhenius law and the rate constants on tray j are

$$k_{Fj} = a_F e^{-E_F/RT_j} \tag{2}$$

$$k_{Bj} = a_B e^{-E_B/RT_j} \tag{3}$$

where a_F and a_B are the preexponential factors, E_F and E_B are the activation energies, and T_j is the absolute temperature on tray j. The reaction rate on tray j can be expressed in terms of mole fractions ($x_{j,i}$) and the kinetic holdups (M_j).

$$R_{j,i} = v_i M_j (k_{Fj} x_{j,A} x_{j,B} - k_{Bj} x_{j,C} x_{j,D}) \tag{4}$$

where $R_{j,i}$ is the reaction rate of component i on the jth tray (mol/s), v_i is the stoichiometric coefficient which takes a negative value for the reactants, and M_j is the kinetic holdup on reactive tray j (mol). Note that kinetic holdup comes from the tray sizing by considering a weir height of 10 cm and the column diameter is determined from the maximum vapor rate by assuming a F-factor of 1. For the case when the reaction occurs in the reboiler and/or the condenser, the maximum kinetic holdup is taken to be 20 times of the tray holdup. In other words, the reactive holdup depends on column geometry and it cannot be set arbitrarily and this is typically true for ion-exchange resin-catalyzed reactions. The overall reactive holdup is transformed into an equivalent catalyst weight and the unit price of Amberlyst 15 is used for cost estimation. It should be noted here that the amount of reactive holdup, consequently the Damkohler number, has important impact to the feasibility and design of RD column.[23,24]

Assumptions made in this work include:

(1) Equimolal reactant feed is assumed, i.e., $F_{OA} = F_{OB}$ where F_{Oi} is the reactant feed flow rate. This implies a "neat" RD design, as opposed to "excess reactant" design.[25]

(2) The forward reaction rate, k_F, is specified as 8 mol/s at 366 K, and the backward rate, k_B, is set to 4 mol/s at the same temperature (i.e., $K_{EQ} = k_F/k_B = 2$ at 366 K). Kinetic and physical property data are given in Table 1.

(3) The kinetics holdup on tray j (M_j) is computed from column geometry by assuming a weir height of 10 cm and kinetics holdups in the reboiler and condenser are taken to be 20 times of tray holdup.

(4) Ideal VLE is assumed, in which constant relative volatilities are used. The tray temperature is computed from bubble point temperature calculation provided with Antoine vapor pressure coefficients (Table 1). That is

$$P = x_{j,A} P^S_{A(T_j)} + x_{j,B} P^S_{B(T_j)} + x_{j,C} P^S_{C(T_j)} + x_{j,D} P^S_{D(T_j)} \tag{5}$$

where P is total pressure and P^S denotes the vapor pressures. Because we will change the boiling point ranking of reactants (A and B) and products (C and D), the Antoine coefficients are given for lighter-than-light key (LLK), light key (LK), heavy key (HK), and heavier-than-heavy key (HHK), and also note that, as a result of constant relative volatility, the Antoine coefficients, B_{VP}'s, are the same for all four components.

(5) The heat of reaction vaporizes some liquid on reactive trays. Therefore the vapor flow rate increases up through the reactive zone, while the liquid flow rate decreases down through the reactive zone.[6] As we count the tray from bottoms up, one obtains:

$$V_j = V_{j-1} - (\lambda/\Delta H_v)R_{j,i} \tag{6}$$

$$L_j = L_{j+1} + (\lambda/\Delta H_v)R_{j,i} \tag{7}$$

where λ is the heat of reaction (-5000 cal/mol) and ΔH_v is the heat of vaporization (6944 cal/mol).

(6) Liquid hydraulic time constant (β) is included by using a linearized form of the Francis weir formulation, and β is set to 6 s.

(7) Vapor holdup and pressure drop are neglected. The dynamic RD model describing material and energy balances is described in detail.[6] The computer code of Kaymak and Luyben[13] is used here with some modification to accommodate process configuration changes. The computer code is programmed in MATLAB m files which can perform economical analysis as the flowsheet converges.

Classification. For a quaternary system (A, B, C, and D), there are 24 (4!) possible boiling point rankings (Figure 1). Here, we use LLK, LK, HK, and HHK to denote the component ranging from the lightest boiler to the heaviest boiler. In terms of relative volatilities, these four boilers can be expressed in the following order.

$$\alpha_{LLK} > \alpha_{LK} > \alpha_{HK} > \alpha_{HHK} \tag{8}$$

Because these two reactants (A and B) are interchangeable and the same applies to the two products (C and D), this leaves us with 6 (24/2/2) possible configurations. Figure 1 shows all 24 possible boiling point rankings and they can be further reduced to six distinct configurations for a quaternary system. According to the *distribution* of reactants and products in relative volatility ranking, we can further classify these six configurations into three types as shown in Table 2.

Type I: One-zone. The first example is that both reactants are LK and HK, and this leaves two products to be LLK and HHK, respectively. In other words, we have: $\alpha_{P_1} > \alpha_{R_1} > \alpha_{R_2} > \alpha_{P_2}$ where P_i stands for the ith product and R_i means the ith reactants. This forms a distinct zone for the reactants in the middle (Table 2). In this case, if the product is the lightest component, it is denoted as type I_p. Similarly, if two products forms one distinct zone (as LK and HK), while having the reactants as the LLK and the HHK, this is also classified as type I. However, if one reactant is the lightest component, it is called type I_r (Table 2). Figure 1 shows four possible scenarios for type I_p and another four possible cases for type I_r. In the subsequent development, we will use $\alpha_C > \alpha_A > \alpha_B > \alpha_D$ to describe type I_p and $\alpha_A > \alpha_C > \alpha_D > \alpha_B$ to represent type I_r.

Type II: Two-zone. The second situation is that the relative volatilities of the two reactants and the two products are adjacent to each other, and this forms two distinct zones for the reactants and the products in the relative volatility ranking as shown in Table 2. The first example is that the products are LLK and LK and two reactants are HK and HHK, respectively, which implies $\alpha_{P_1} > \alpha_P > \alpha_{R_1} > \alpha_{R_2}$. Because one of the products is the lightest component, it is denoted as type II_p. Figure 1 shows four possible scenarios for type II_p, and we use $\alpha_C > \alpha_D > \alpha_A > \alpha_B$ to represent this type. On the contrary, if the reactants are LLK and LK and two products are HK and HHK, we have type II_r. Table 2 shows type II_r with two distinct zones in the relative volatility ranking. Here, we use $\alpha_A > \alpha_B > \alpha_C > \alpha_D$ to describe type II_r.

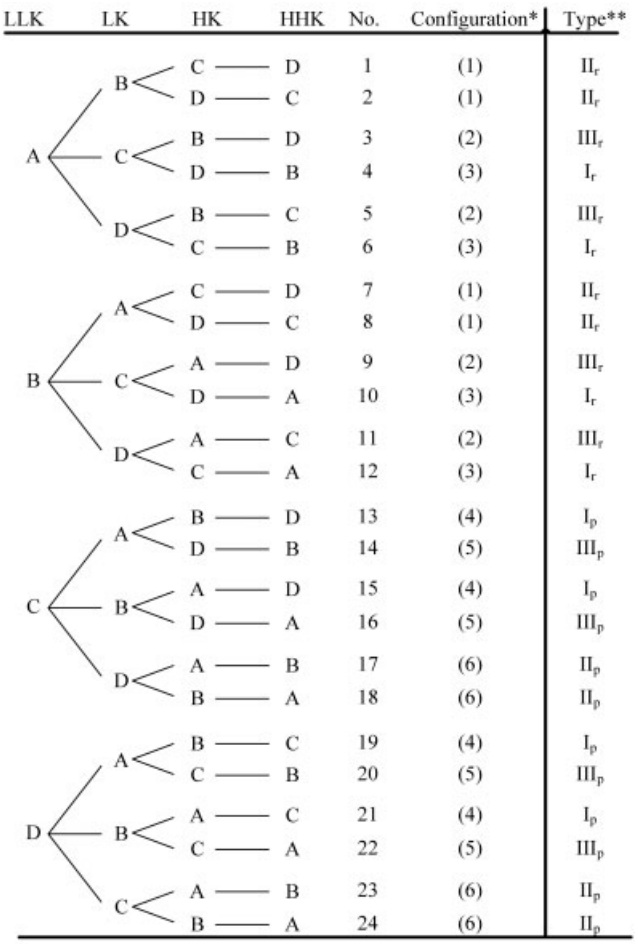

Figure 1. All 24 possible boiling point rankings, 6 distinct configurations, and 3 process types for possible reactant/product relative volatilities distribution.

Type III: Alternating. The third type corresponds to the situation when the relative volatility ranking is arranged in an alternating manner for the reactants and the products as shown in Table 2. For example, if the sequence of the relative volatility in a descending order is: product 1, reactant 1, product 2, and reactant 2 (i.e., $\alpha_{P_1} > \alpha_{R_1} > \alpha_{P_2} > \alpha_{R_2}$), we have the case of type III_p. Figure 1 shows four possible cases for type III_p, and, we use $\alpha_C > \alpha_A > \alpha_D > \alpha_B$ to represent it. On the contrary, if the reactants are LLK and HK and two products are LK and HHK, we have type III_r. Table 2 shows four possible combinations for type III_r, and, here, we use $\alpha_A > \alpha_C > \alpha_B > \alpha_D$ to represent type III_r.

Relaxation and convergence. Before leaving the section, we would like to address some simulation and convergence issues in the design of RD as process configuration changes. The relaxation approach[23,25] is taken here. For a given RD design (e.g., number

Table 2. Classification for Process Types

Reaction R1 + R2 ⇔ P1 + P2		
Type I (one-zone)	I_p	$\alpha_{P_1} > \alpha_{R_1} > \alpha_{R_2} > \alpha_{P_2}$
	I_r	$\alpha_{R_1} > \alpha_{P_1} > \alpha_{P_2} > \alpha_{R_2}$
Type II (two-zone)	II_p	$\alpha_{P_1} > \alpha_{P_2} > \alpha_{R_1} > \alpha_{R_2}$
	II_r	$\alpha_{R_1} > \alpha_{R_2} > \alpha_{P_1} > \alpha_{P_2}$
Type III (alternating)	III_p	$\alpha_{P_1} > \alpha_{R_1} > \alpha_{P_2} > \alpha_{R_2}$
	III_r	$\alpha_{P_1} > \alpha_{P_2} > \alpha_{R_2} > \alpha_{P_2}$

of reactive, rectifying, and stripping trays, feed flow rates, and feed tray locations), a control system is set up to drive the process toward the design specifications. Given the initial guesses in tray compositions, the set of ordinary differential equations is integrated from the initial condition until a steady state is reached. It should be emphasized here that, the control structure for relaxation is very different the one in control practice. The reason is that perfect flow control can be achieved in simulation, no stoichiometric imbalance. For example, for the type I system with the product as the lightest component, type I_p, all four external flows (inlet and outlet streams) are under flow control, the product composition is controlled by adjusting the reflux flow (internal flow), and the bottoms level is maintained by changing vapor boilup as shown in Figure 2A. In other words, given the feeds, two control degrees of freedom is the distillate composition and distillate flow rate. Another example is also a type I system, but one of the reactant is the lightest component, type I_r. This leads to a rather unconventional RD column, as will be explained later, and the product is withdrawn from the middle of the column as a liquid side-stream. Figure 2B shows the control structure to obtain the steady-state condition. Again, two feeds are under flow control, the product composition is controlled by adjusting vapor boilup, reflux drum level is maintained by changing the reflux flow, and base level is controlled by the side-draw flow rate. Again, this type of control structure will never be implemented in practice because of assumption of perfect flow control. Given two feeds, this system has only one control degree of freedom, side-stream composition. A convergence criterion is used to verify the steady-state condition. In this work, the following criterion is used.

$$\varepsilon = \max\left(\left|x_{B,i}^{k} - x_{B,i}^{k-1}\right|, \left|x_{j,i}^{k} - x_{j,i}^{k-1}\right|, \left|x_{D,i}^{k} - x_{D,i}^{k-1}\right|\right) < 10^{-4} \quad \forall i = 1, \mathrm{NC}\ \forall j = 1, \mathrm{NT} \qquad (9)$$

where $x_{j,i}$ denotes the ith component on the jth tray, $x_{B,i}$ is the bottoms composition for the ith component, $x_{D,i}$ is the distillate composition of the ith component, NC represents the number of components, NT stands for total number of trays, and the superscript k means the discrete-time index. For the given convergence criterion with an integration step sized of 1 s, it takes 7 h (process time as shown in Figure 3A) to converge a type I_p (Figure 2A) flowsheet and this corresponds a CPU time of 69 s on a Pentium 4 PC. For the difficult RD process, I_r, shown in Figure 2B, it takes 160 h to meet convergence criterion. Figure 3B shows extremely slow composition dynamics in side-stream composition. Again, this corresponds a CPU time of 1800 s on a Pentium 4 PC. Moreover, in many cases, flowsheet may not converge after 200 h, if the initial guesses are not appropriate. Appendix A shows the effects of initial conditions to the convergence for two different process configurations. For the control part, little improvement in the speed of convergence even variable gain controllers are used, e.g., using larger controller gain as the error becomes smaller. The results presented here clearly indicate that the simulation of RD systems remains a very difficult problem, and, frequently, it fails to converge. Unless further improvement in the numerical simulation is made, automated design via mathematical programming is very difficult, if not impossible.

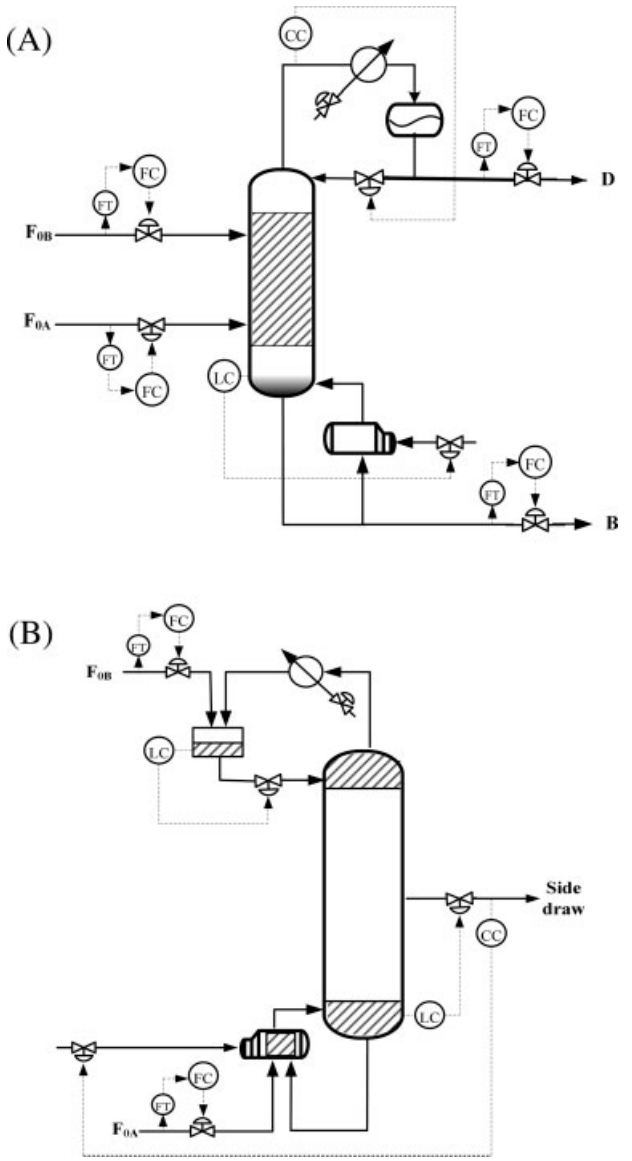

Figure 2. Control structure used for dynamic simulation using relaxation for (A) type I_p: LK + HK ⇔ LLK + HHK and (B) type I_r: LLK + HHK ⇔ LK + HK.

Process configurations

Before getting into exploring process configuration, the design procedure is outlined first. The design variables (e.g., location of reactive zone, tray numbers, feed locations, etc.) are identified first and then all combinations are exhausted to find the finalized design.[19] The objective function for design is the total annual cost (TAC) and the specifications are 95% purity level

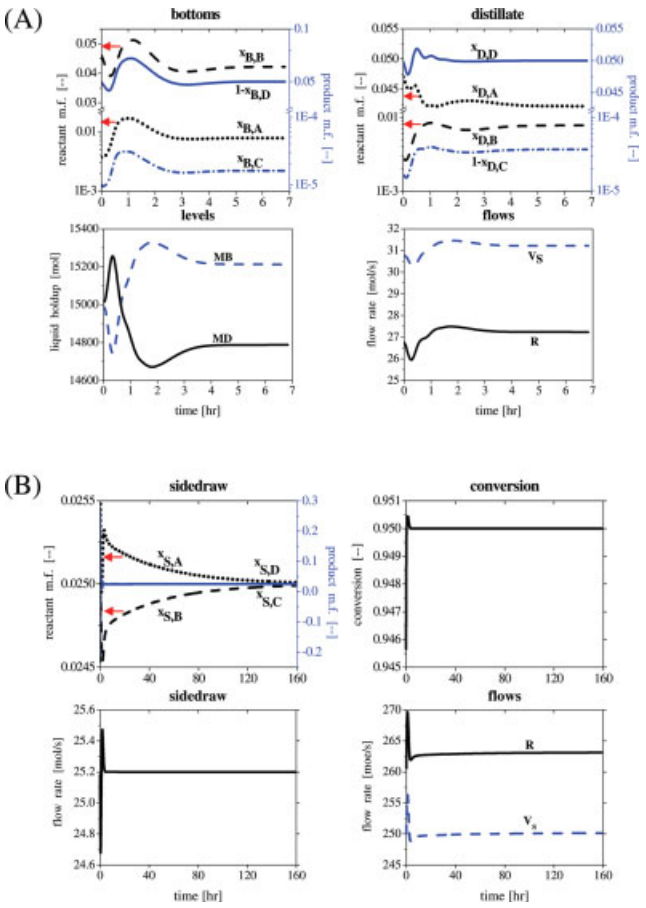

Figure 3. Converging dynamic simulation using relaxation for (A) type I_p: LK + HK ⇔ LLK + HHK and (B) type I_r: LLK + HHK ⇔ LK + HK.

[Color figure can be viewed in the online issue, which is available at www.interscience.wiley.com.]

for the products. The design problem can be formulated as

$$\begin{aligned} &\underset{X}{\text{Minimize}}\ \text{TAC} \\ &\text{Subject to } x_{\text{product,C}} \geq 0.95 \\ &\qquad\qquad x_{\text{product,D}} \geq 0.95 \end{aligned} \tag{10}$$

where X is the vector of design variables and the TAC is defined as

$$\text{TAC} = \text{Operating cost} + \frac{\text{Capital cost}}{\text{Payback year}} \tag{11}$$

Here, a payback year of 3 is used. The formula for the TAC computation is taken from Kaymak and Luyben.[12] As a result of different relative volatility rankings, process configurations may vary from one column to two columns with different product withdraw location. Here, we use a type I example, type I_p, to illustrate the design procedure.

$$\begin{aligned} &\text{A} + \text{B} \Leftrightarrow \text{C} + \text{D} \\ &\text{LK}\ \ \text{HK}\ \ \text{LLK}\ \ \text{HHK} \end{aligned} \tag{12}$$

Given the product specification, design variables include the number of reactive trays (N_{rxn}), the numbers of rectifying and stripping trays (N_R and N_S), and feed tray locations for the heavy and light reactants (NF_{heavy} and NF_{light}). Instead of blindly exhausting all possible combinations of design variables, a systematic design procedure is used. It should be emphasized here that process knowledge is needed to place the reactive zone(s) and a simple rule is: place the reactive zone(s) at where the reactants are most *abundant*. For the type I_p, process, it is located at the mid-section of the column.

(1) Set the reactants feed ratio to 1 (i.e., $FR = F_{light}/F_{heavy} = 1$).

(2) Place the reactive zone in the *mid-section* of the column and fix the number of reactive trays (N_{rxn}).

(3) Place the heavy reactant feed (NF_{heavy}) on the top of the reactive zone and introduce the light reactant feed (NF_{light}) on the lowest tray of the reactive zone.

(4) Guess the number of trays in the rectifying section (N_R) and the stripping section (N_S).

(5) Perform simulation using dynamic model with feedback control to meet the product specification.

(6) Return to step 4 and change N_R and N_S until the TAC is minimized.

(7) Return to step 3 and find the feed locations (NF_{heavy} and NF_{light}) until the TAC is minimized.

(8) Return to step 2 and vary N_{rxn} until the TAC is minimized.

Type I: One-zone. *Type I_p: LK + HK = LLK + HHK*. This is the most popular RD configuration, studied by a number of authors.[6,12,13,16] In real chemical systems, the production of diphenyl carbonate belongs to this class.[26] The *net* reaction can be expressed as

$$\begin{aligned} &\text{Dimethyl carbonate} + 2\ \text{Phenol} \Leftrightarrow 2\ \text{Methanol} + \text{Diphenyl carbonate} \\ &\qquad\text{LK}\qquad\qquad\text{HK}\qquad\qquad\text{LLK}\qquad\qquad\text{HHK} \end{aligned}$$

It should be noted here that many real chemical systems have azeotropes associated with quaternary system and it may make the neat RD design infeasible. But for the real chemical systems illustrated here, the placement of the reactive zone are the same as that of the ideal systems, despite having azeotropes. The boiling point ranking leads to easy separation between the reactants and products. The two products leave the reactive section from the opposite sides of the reactive zone while two intermediate boilers (the reactants) are kept in the reactive zone. This is the most favorable boiling point arrangement for a RD system.

Figure 4A shows the effects of separation trays and reactive trays on the TAC. Because of the symmetry in the two products, the numbers of trays in the rectifying section and in the stripping section are assumed to be the same, i.e., $N_R = N_S$. Figure 4A indicates that optima exist for the number of reactive trays ($N_{rxn} = 16$) and number of separation trays ($N_R = N_S = 4$). The tradeoff comes from the fact that, at the vicinity of the optimum, the operating cost goes down and the capital cost goes up, as we increase number of separation trays. Figure 4B shows that the TAC is quite sensitive to feed tray locations which is consistent with the previous findings.[16,20] When the heavy reactant feed and light reactant feed are five trays apart, the design gives lower TAC and the optimum corresponds to $NF_{heavy} = 16$ and $NF_{light} = 11$. This results in a TAC of \$254,170 and the detailed process flowsheet is given in Table 3.

Figure 5 shows that, for type I_p, RD with products as the LLK and HHK, the reactive zone is located at the middle of the column and the light product (LLK) and the heavy product (HHK) are removed from the top and bottoms of the column,

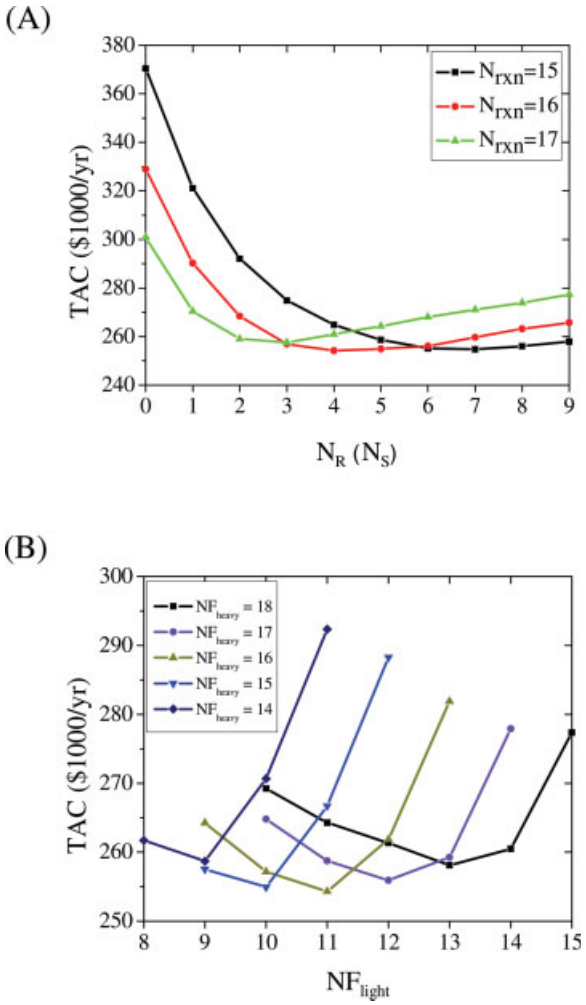

Figure 4. Relationship between TAC and design variables for type I_p process: (A) number of separation trays (N_R & N_S) versus TAC for different N_{rxn} and (B) feed tray locations (NF_{heavy} & NF_{light}) with N_{rxn} = 22 and $N_R(N_S)$ = 4.

[Color figure can be viewed in the online issue, which is available at www.interscience.wiley.com.].

respectively. This is intuitively correct, because we have higher reactants (intermediate boilers) composition in the mid-section of the column. As will become clear later, one of the most important elements in the conceptual design of RD is placing the reactive zone at the right location. The composition profile of the final design is given in Figure 6 and, as expected, significant amount of reactants are presented in the reactive zone (between two dashed lines) and product compositions increase gradually toward top and bottoms of the column. Figure 6 also reveals the fraction of total conversion (R_i/R_t) in each reactive tray and results indicate that all reactive trays are well utilized in the reactive zone.

Before leaving the section, we explore the effects of reactive holdups to the designs (assumption 3 in design). The weir height is varied from 5 to 40 cm (very likely the lower and upper limits for real columns) and Figure 7 shows that the TAC changes from −10% (5 cm) to + 10% (40 cm). Instead of using two extreme values, in this work, a modest weir height, 10 cm, is taken.

Type I_r: LLK + HHK = LK + HK. This corresponds to the following reaction:

$$\begin{array}{c} A + B \Leftrightarrow C + D \\ \text{LLK HHK LK HK} \end{array} \tag{13}$$

The boiling point ranking clearly indicates that this is a very difficult RD system, because large amount of reactants A and B can hardly coexist in the liquid phase (one is the LLK and the other is the HHK) and this is the worst case scenario for the forward reaction (extreme favorable for the backward reaction). In the production of bio-based esters, many processes fall into belongs to this class. A typical example is the recovery of lactic acid.[27] The reaction can be expressed as

$$\begin{array}{c} \text{Methanol} + \text{Lactic acid} \Leftrightarrow \text{Water} + \text{Methyl lactate} \\ \text{LLK} \qquad \text{HHK} \qquad \text{LK} \qquad \text{HK} \end{array}$$

Unless, one can consume all the HHK toward the bottoms and react away all the LLK toward the top of the RD, single column configuration (e.g., Figure 5) is not possible and this is typically true for the "neat" design. A more likely configuration is placing the reactive zones at the opposite ends of the column where significant amount of LLK and HHK (two reactants) are presents. Then, the heavy reactant (HHK) is introduced into top of the column where significant amount of the other reactant (LLK) is present. Similarly, the light reactant (LLK) is fed to the bottoms of the column where significant amount of the heavy reactant (HHK) is present (Figure 8). The next question then becomes: how to withdraw the product? The answer is actually quite simple, as a side stream from the RD column with a mixture of two products. Thus, we need an additional column to separate these two products. Once correct process configuration is set, design variables are easily identified. They are number of reactive stages at two different zones, number of separation trays, and side draw location. Note that feed locations shown in Figure 8 are actually the optimal ones and we will not show the effect of feed tray locations in design for type I_r. Also note here that the separation column is designed by setting the total number of trays to two times of the minimum number of trays, i.e., N_T=2N_{min}. Again, the sequential design procedure is applied and, for the sake of clarity, detailed design steps and corresponding costs are given in Appendix B.

Figure 8 gives the process flowsheet and parameter values are given in Table 3. This flowsheet results in a TAC of $1,575,930 which is 620% of that of type I_p system. The reason is that, in order to achieve high conversion, the reflux to feed ratio in the RD is extremely high, 20.5, and the vapor boilup to feed ratio is 19.1. This corresponds to a column of 30 trays where the reactive zones are located at the top and bottoms of the column with reactive holdups of 20 and 1 times of tray reactive holdup in the condenser and reboiler, respectively. Because the catalyst cost is also included in the TAC calculation, the kinetic holdups in the reboiler and condenser, in theory, are also design variables (not exceeding 20 times of tray holdup). In this case, the reboiler kinetic holdup is varied to minimize the TAC. A mixture of two products (LK and HK) is withdrawn from the middle of separation section (tray 14)

Table 3. Final Design for All Six Process Flowsheets

System	I_p	I_r		II_p		II_r		III_p	III_r
Column configuration	RD	RD	*SD*	RD	*SD*	RD	*SD*	RD	RD
Total no. of trays	24	32	48	11	54	28	62	59	96
No. of trays in stripping section (N_S)	4					3		2	35
No. of trays in reactive section (N_{rxn})	16	2[a] + 4[b]		6[a]		25[b]		49	57
No. of trays in rectifying section (N_R)	4			5				8	4
Reactive trays	5–20	0–1;27–32		0–5		4–28		9–57	5–61
Heavy reactant feed tray (NF_{heavy})	11	32		0		28		57	55
Light reactant feed tray (NF_{light})	16	0		0		4		46	5
Heavy reactant feed flow rate (kmol/h)	45.36	45.36		45.36		45.36		45.36	45.36
Light reactant feed flow rate (kmol/h)	45.36	45.36		45.36		45.36		45.36	45.36
Top product flow rate (kmol/h)	45.36		45.36	90.72	45.36		45.36	45.36	45.36
Bottom product flow rate (kmol/h)	45.36		45.36		45.36	90.72	45.36	45.36	45.36
Reflux flow rate (kmol/h)	95.15	931.03	94.32	93.71	97.884	446.18	102.38	99.40	270.68
Vapor boilup rate (kmol/h)	109.45	881.28	139.68	152.57	143.25	368.53	147.71	113.72	285.05
Column diameter (m)	0.692	1.740	0.700	0.801	0.698	1.136	0.733	0.702	1.053
Weir height (m)	0.100	0.100	0.100	0.100	0.100	0.100	0.100	0.100	0.100
Condenser heat transfer area (m^2)	96.75	603.95	95.26	125.76	97.69	256.33	100.74	98.74	215.53
Reboiler heat transfer area (m^2)	45.27	360.06	57.07	62.34	58.53	150.57	60.36	46.47	116.46
Total capital cost ($1000)	349.45	1198.52	457.83	346.30	482.52	686.91	529.76	488.54	988.36
Column	119.13	379.03	209.34	68.64	229.30	221.02	269.87	247.90	564.00
Column trays	3.12	16.21	6.32	1.62	7.08	7.53	8.77	7.81	23.82
Heat exchangers	227.83	803.29	242.16	276.03	246.15	458.35	251.12	232.83	400.54
Total operating cost ($1000/year)	137.68	1176.4	167.22	207.80	171.47	513.16	176.83	157.24	396.35
Catalyst	6.68	121.53		25.16		72.03		21.10	55.15
Energy	131.01	1054.9	167.22	182.63	171.47	441.14	176.83	136.14	341.20
TAC ($1000/year)	254.17	1575.9	319.90	323.23	332.31	742.13	353.41	320.08	725.80
TAC (entire process; $1000/yr)	254.17	1895.8		655.54		1095.5		320.08	725.80

RD, reactive distillation column; SD, simple distillation column.
[a]Including a reactive reboiler.
[b]Including a reactive condenser.

which is subsequently fed into a simple distillation column. The second column has a total of 48 trays with moderate reflux ratio (RR) and boilup ratio (BR), RR = 2.08 and BR = 3.08. Figure 9A shows the composition profile for the reactants (A and B) and products (C and D). As expected, concentrations of two reactants are drastically different in the reactive zones. For example, the LLK (A) exceed 60% toward the top reactive zone while the concentration of the heavy reactant (HHK, B) remains below 2%, despite the fresh feed of HHK is introduced in the condenser, and a similar behavior is observed in the lower reactive zone. At the side-draw location, the compositions of both products are the same (stoichiometric balance) as shown in Figure 9A. The product stream is fed to a distillation column for further separation to obtain 95% C and D. Figure 9B shows the composition profile of the distillation column with rather symmetric profiles.

Type II: Two-zone. *Type II_p: HK + HHK = LLK + LK.* This corresponds to the following reaction:

$$\begin{array}{c} A + B \Leftrightarrow C + D \\ HK\ \ HHK\ \ LLK\ \ LK \end{array} \qquad (14)$$

The boiling point ranking indicates that both reactants (A and B) are heavier than the products (C and D). These two reactants are more concentrated toward the lower part of the RD column while the two products can be separated easily from the top of the column. Following the rule of "placing the reactive zone at location with high reactant concentration," the lower section of the column should be made reactive while the separation is carried out in the upper section of the column. This leads to the RD configuration in Figure 10. This configuration actually is quite similar to that of ethyl acetate and isopropyl acetate RD columns. The overhead product of the RD column is then fed to a simple distillation column to separate two products. Because the impurity (unreacted reactants) is one-sided

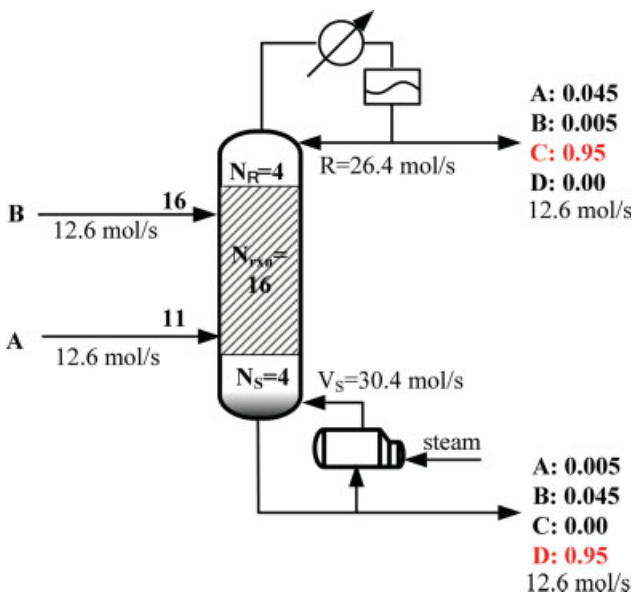

Figure 5. Final design for type I_p process (LK + HK ⇔ LLK + HHK).

[Color figure can be viewed in the online issue, which is available at www.interscience.wiley.com.]

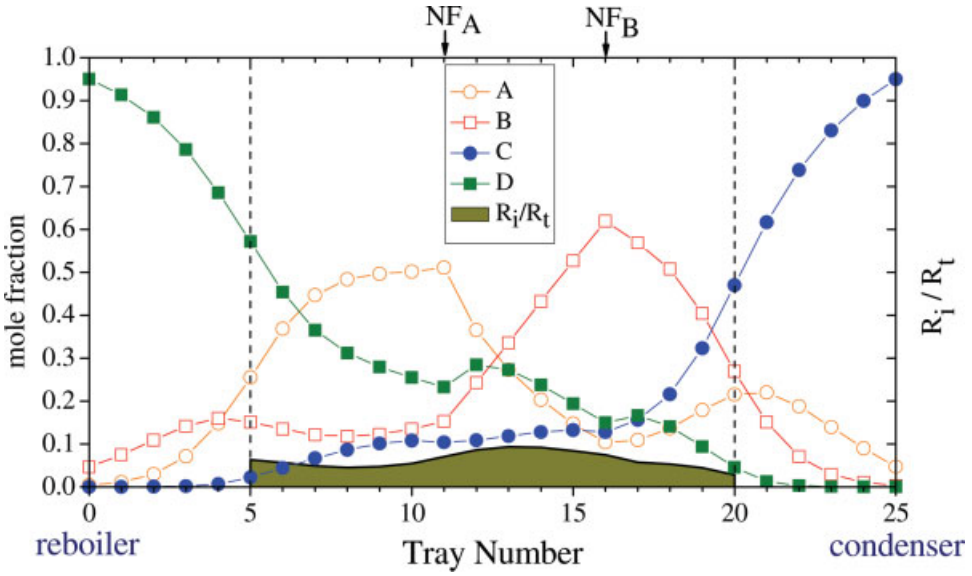

Figure 6. Composition profile, feed locations, and fraction of total conversion (R_i/R_t) for type I_p process (LK + HK ⇔ LLK + HHK).

[Color figure can be viewed in the online issue, which is available at www.interscience.wiley.com.]

(heavier than two products), in order to keep product compositions no less than 95%, the conversion in the RD column should be greater than 95% (97.5% in this case). This results in the following product composition 95% D (LK) and 97.5% C (LLK). Again, the design procedure is applied and Figure 10 gives and final design where the TAC is minimized. For the sake of clarity, the relationship between the TACs and design variables is illustrated in Appendix B. Table 3 gives the parameter values of this design.

The flowsheet gives a TAC of $655,000 which is 158% higher than that of type I_p. The TAC of the RD column is $363,000 which is slightly higher than that of (TAC = $254,000). This gives a RD of five reactive trays plus a reactive reboiler and five rectifying trays. The vapor boilup to feeds ratio is around 2 and the reflux ratio is close to 1. Actually, this is a relatively simple RD column with reasonable energy consumption and the explanation for that is: the reaction takes place in the *high* temperature zone of the column and we have an excessive large reactive holdup (the holdup in the reboiler is 20 times of tray reactive holdup) when the temperature is highest. In other words, the location of the reactive zone (Figure 10) facilitates the reactive separation. Figure 11A confirms that most of the conversion takes place in the reboiler and the remaining reactive trays carry the reaction further to the desired conversion. The reactant composition of the HHK (B) is kept high in the reactive zone and the other reactant A (HK) is maintained at an almost constant level to ensure the forward reaction is dominate. Toward the top of the RD column two light products are purified further and subsequent separation (Figure 11A). The TAC of the second column ($332,000) is about the same as that of the RD column. This is a simple distillation with heavy impurities. Thus the bottoms composition is kept to the specification, 95% of D (LK) while the top product gives a composition of 97.5% D with 2.5% C as impurity. This column has 54 trays and the feed is introduced into tray 43. The distillation column has a moderate energy consumption with a boilup ratio is 3.36 and a reflux ratio of 2.07. Figure 11B shows the composition profile in the distillation column where the two unreacted (heavy) reactants walk their way toward the bottoms of the column.

Type II_r: LLK + LK = HK + HHK: This corresponds to the following reaction:

$$\begin{array}{c} A + B \Leftrightarrow C + D \\ \text{LLK LK HK HHK} \end{array} \qquad (15)$$

In terms of reactants and products, the boiling point ranking is just the opposite of type II_p (Eq. 15 versus Eq. 14) where the

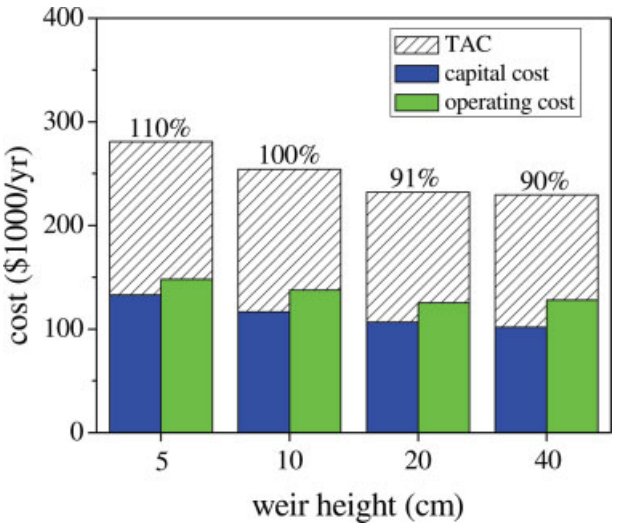

Figure 7. Effects of weir height (reactive holdup) to the TAC with weir height of 10 cm as the base case.

[Color figure can be viewed in the online issue, which is available at www.interscience.wiley.com.]

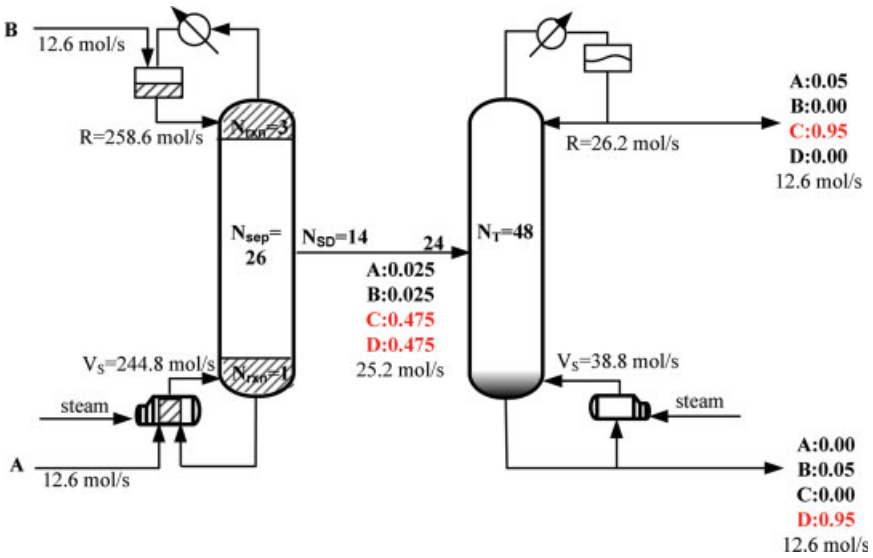

Figure 8. Final design for type I_r process (LLK + HHK ⇔ LK + HK).

[Color figure can be viewed in the online issue, which is available at www.interscience.wiley.com.]

two reactants are lighter than two products. Thus, these two reactants are more concentrated toward the upper part of the RD column while the two products can be withdrawn from the bottoms of the column. A typical example is the acetalization reaction for the synthesis of ethylal.[28] The reaction can be expressed as

$$\underset{\text{LLK}}{\text{Formaldehyde}} + \underset{\text{LK}}{\text{Ethanol}} \Leftrightarrow \underset{\text{HK}}{\text{Ethylal}} + \underset{\text{HHK}}{\text{Water}}$$

So, the upper section of the column should be made reactive while the separation is carried out in the stripping section. This gives a RD configuration shown in Figure 12. The reaction takes place in the RD column and the bottoms product is then fed to a simple distillation column to separate two products. Because two unreacted reactants (LLK and LK) is heavier than two products (HK and HHK), the conversion in the RD column is set to 97.5% such that both product, HK in particular, can meet the 95% specification. The product compositions are 95% C (HK), along with two light reactants, and 97.5% D (HHK), along with 2.5% HK (C). Following the design procedure, the final design is shown in Figure 12. Table 3 gives the parameter values of this design.

Intuitively, this process looks as if the mirror image of type II_p where the reactants and two products switch side. However, the flowsheet gives a TAC of \$1,096,000 which is 150% of that of type II_p and, moreover, the TAC of the RD column is \$742,000 which is twice the cost of the RD for type II_p (TAC = \$323,000). The reason for that is actually quite simple: the reaction takes place in the *low* temperature zone (upper section of the column). This leads to a RD of 24 reactive trays plus a reactive condenser and 3 stripping trays. As expected, the LK (D) is introduced into the condenser while the LLK (C) is fed into the reactive zone 9 trays below (Figure 12). The reflux to feeds ratio is around 4 and the boilup ratio is also close to 4. These values are much higher than that of type II_p, so is the energy consumption in the RD column. This example illustrates the conflict between reactant concentration and reaction temperature in a chemical reaction and this is a unique feature of RD. Because of the reversible reaction, the reactive zone is placed at where the reactants are most abundant and this leads to the upper section of the RD column which is the low temperature zone. It is interesting to note that the reaction temperature is the lowest (reflux drum) when the product of two reactant concentration is the highest. Figure 13A indicates that most of a significant portion of the reaction takes place in the condenser and the remaining reactive trays carry the reaction further to the desired specification. The composition profile is qualitatively similar to that of II_p, except the reactive zone is much longer. Toward the bottoms of the RD column, two heavy products reach 48.75% with 2.5% of unreacted reactants. The TAC of the second column (\$353,000) is only half of that of the RD column. This is a simple distillation with light impurities and the reflux ratio is around 2 and the boilup ratio is a little higher than 3. Thus the top composition is kept to the specification, 95% of D (LK) while the bottoms composition is 97.5% D with 2.5% C as impurity. This column has 62 trays and the feed is introduced into tray 11. Figure 13B shows the composition profile in the distillation column and the two unreacted (light) reactants end up on the top of the column.

Type III: Alternating. *Type III_p: LK + HHK = LLK + HK.* When one of the products (C) is the lightest component, we have the following reaction:

$$\underset{\text{LK}}{\text{A}} + \underset{\text{HHK}}{\text{B}} \Leftrightarrow \underset{\text{LLK}}{\text{C}} + \underset{\text{HK}}{\text{D}} \qquad (16)$$

The boiling point ranking indicates that if we consume the heavy reactant (the HHK B) toward the bottoms of the column, the heavy product (the HK D) can be obtained from the column base. The scenario is simpler toward the top of the column,

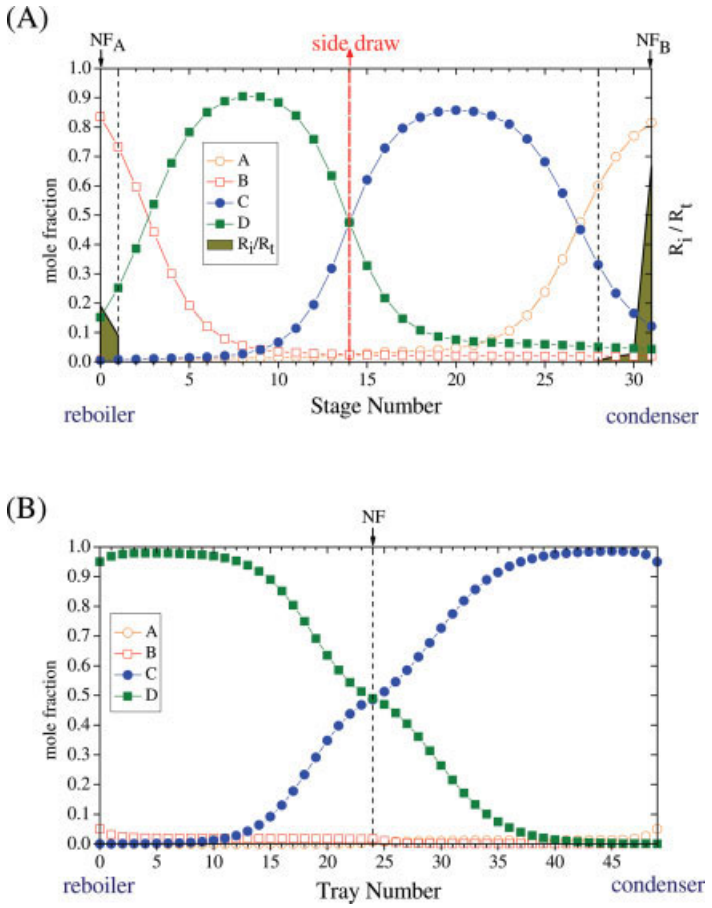

Figure 9. Composition profile, feed locations, and fraction of total conversion (R_i/R_t) for type I_r process (LLK + HHK ⇔ LK + HK) in (A) reactive distillation column and (B) simple distillation column.

[Color figure can be viewed in the online issue, which is available at www.interscience.wiley.com.]

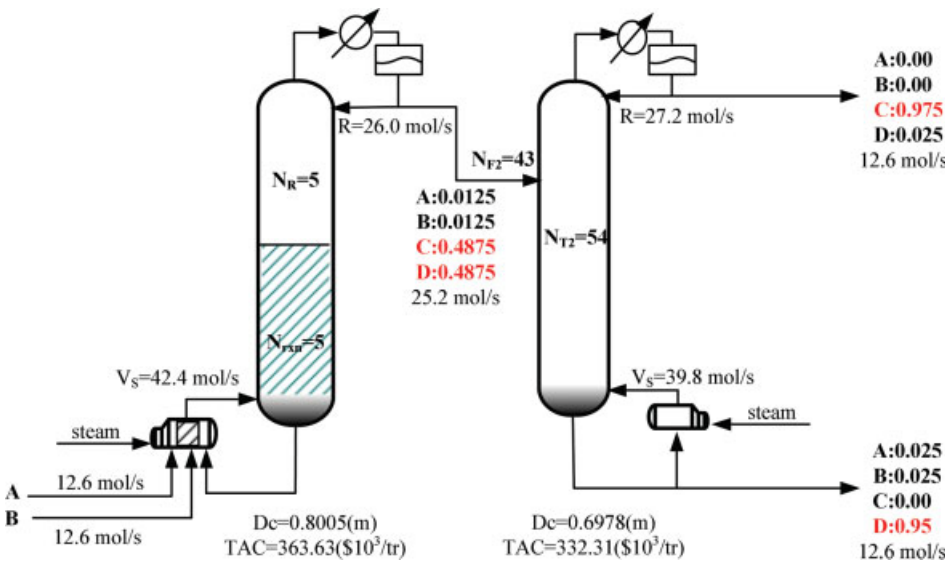

Figure 10. Final design for type II_p process (HK + HHK ⇔ LLK + LK).

[Color figure can be viewed in the online issue, which is available at www.interscience.wiley.com.]

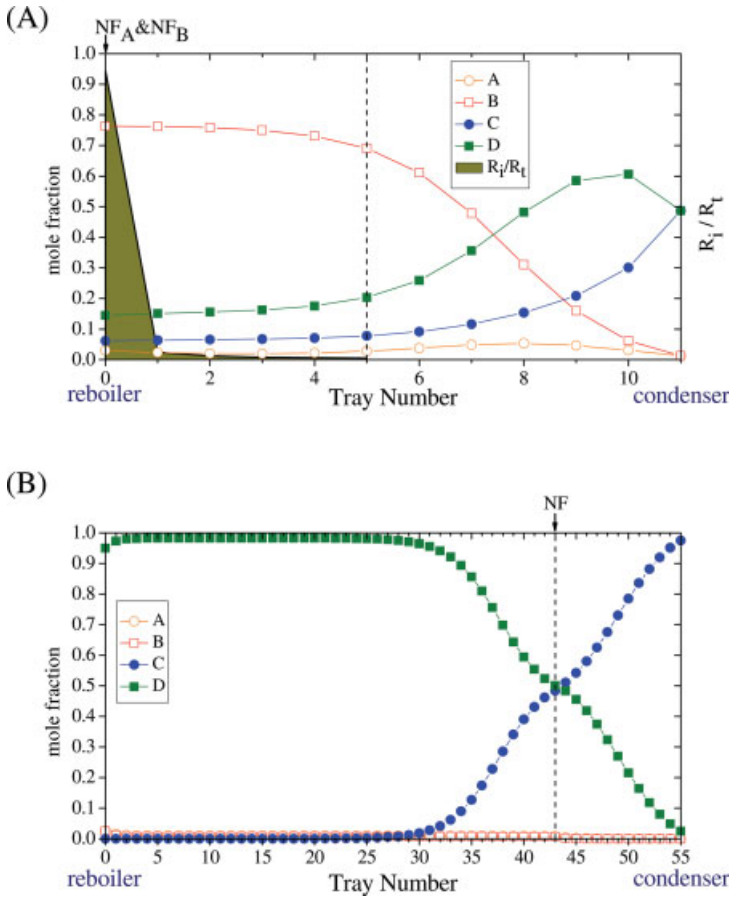

Figure 11. Composition profile, feed locations, and fraction of total conversion (R_i/R_t) for type II_p process (HK + HHK ⇔ LLK + LK) in (A) reactive distillation column and (B) simple distillation column.

[Color figure can be viewed in the online issue, which is available at www.interscience.wiley.com.]

because, the light reactant (the LLK C) can be withdrawn easier from the top. The popular methyl acetate production via acetic acid esterification[19] example falls into this category.

$$\underset{\text{LK}}{\text{Methanol}} + \underset{\text{HHK}}{\text{Acetic acid}} \Leftrightarrow \underset{\text{LLK}}{\text{Methyl acetate}} + \underset{\text{HK}}{\text{Water}} \quad (17)$$

Because two products are withdrawn from the opposite ends of the column, the reactive zone is placed in the middle. This column configuration is shown in Figure 14. Appendix B illustrates the design procedure where effects of design variables on the TAC can be clearly seen. Table 3 gives the parameter values of this design.

The flowsheet gives a TAC of $321,000 which is the second lowest in all 6 cases (126% of that of type I_p). The RD column has a total of 59 trays with 49 reactive trays, 8 stripping trays and 2 rectifying trays. Two feeds (11 trays apart) are introduced into the upper section of the reactive trays as shown in Figure 14. Both the reflux ratio and boilup ratio are a little greater than 2. Actually, this is a relatively simple RD column with moderate energy consumption, despite having relatively large number of reactive trays. Having one reactant being the HHK (reactant B) has its advantages and disadvantage. The HHK increases the tray temperature when we have significant amount of this heavy reactant which is advantageous for the reaction and this is shown in Figure 15B. The down side is that we have to react away almost all of the HHK in the reactive zone (otherwise it will end up in the column base), and this leads to excessive large number of reactive trays. This is clearly illustrated in Figure 15A where we have very small amount of conversion between tray 9 and tray 40. The purpose for this portion of reactive trays is rather to consume the remaining heavy reactant (the HHK B) than to generate more products. The reactant composition of the LK (A) is kept fairly constant below the feed point to ensure the dominance of the forward reaction (Figure 15A). The two products are further purified toward the top and bottoms of the RD column to meet the specification.

Type III_r: LLK + HK = LK + HHK: For alternating type, when one of the reactant (A) is the lightest component, we have the following reaction:

$$\underset{\text{LLK}}{\text{A}} + \underset{\text{HK}}{\text{B}} \Leftrightarrow \underset{\text{LK}}{\text{C}} + \underset{\text{HHK}}{\text{D}} \quad (18)$$

The boiling point ranking suggests that if we consume the light reactant (the LLK A) toward the top of the column, the light product (the LK C) can be obtained from the column overhead. The scenario is simpler toward the bottoms of the column,

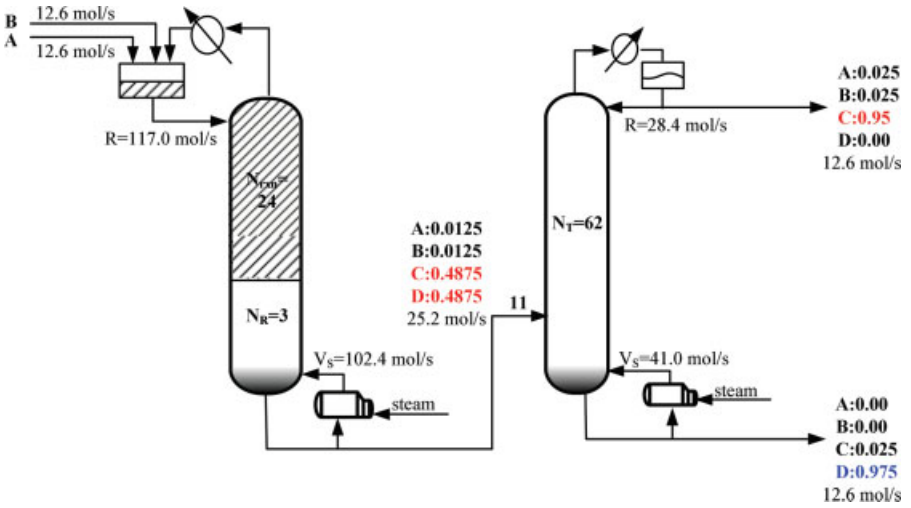

Figure 12. Final design for type II$_r$ process (LLK + LK ⇔ HK + HHK).

[Color figure can be viewed in the online issue, which is available at www.interscience.wiley.com.]

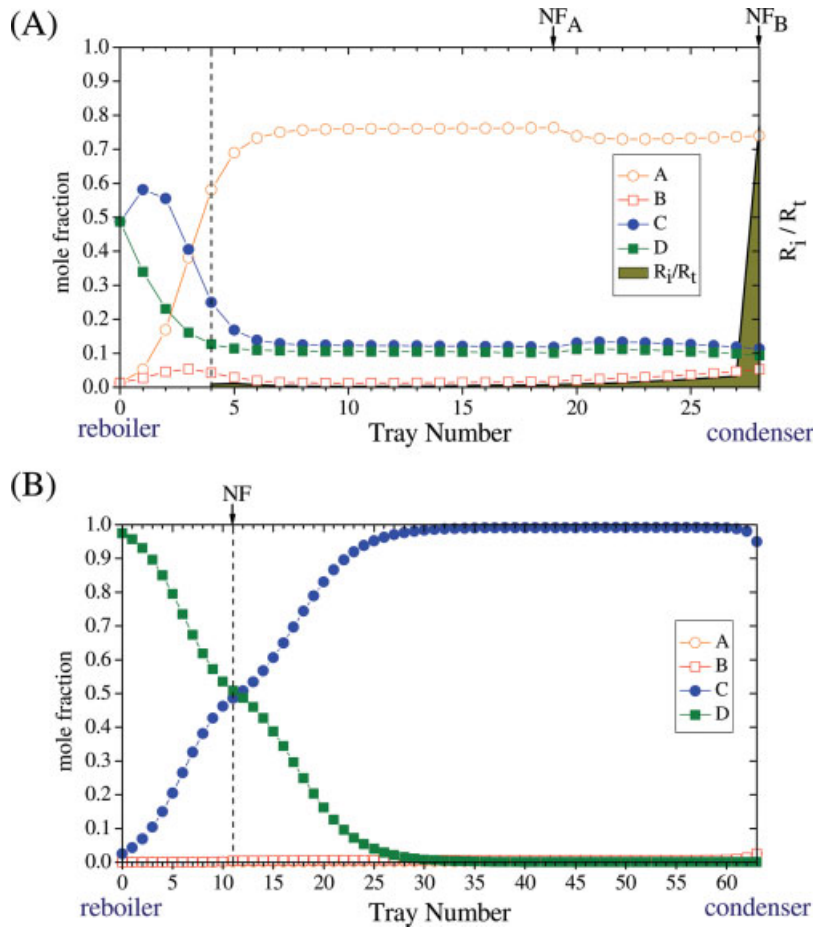

Figure 13. Composition profile, feed locations, and fraction of total conversion (R_i/R_t) for type II$_r$ process (LLK + LK ⇔ HK + HHK) in (A) reactive distillation column and (B) simple distillation column.

[Color figure can be viewed in the online issue, which is available at www.interscience.wiley.com.]

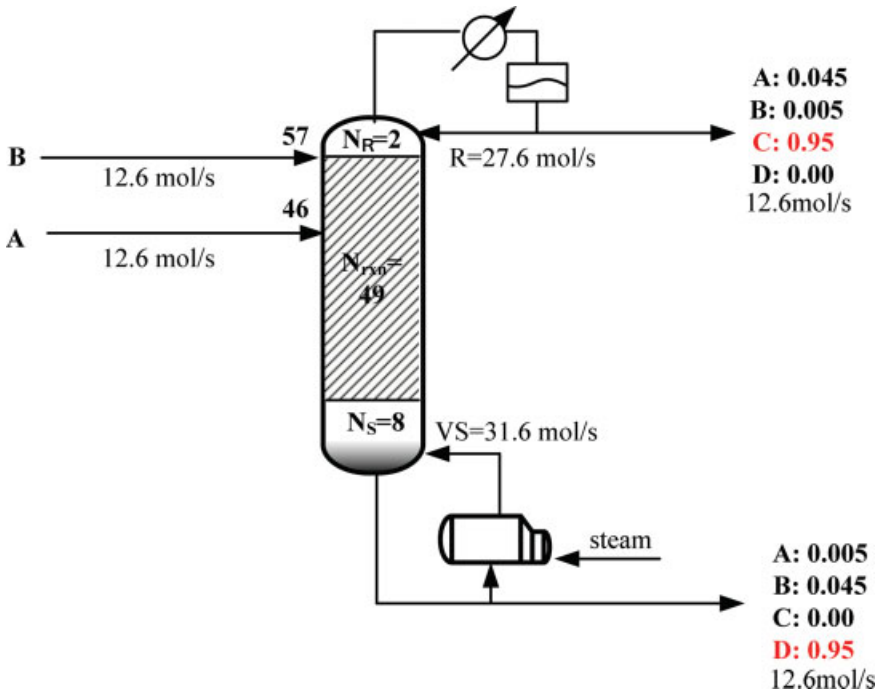

Figure 14. Final design for type III_p process (LK + HHK ⇔ LLK + HK).

[Color figure can be viewed in the online issue, which is available at www.interscience.wiley.com.]

because, the heavy reactant (the HHK D) can be separated easily from the heavy reactant (the HK B). The methyl acetate hydrolysis[3] is a typical example.

$$\underset{\text{LLK}}{\text{Methyl acetate}} + \underset{\text{HK}}{\text{Water}} \Leftrightarrow \underset{\text{LK}}{\text{Methanol}} + \underset{\text{HHK}}{\text{Acetic acid}} \quad (19)$$

It should be emphasized here that the "neat" design is considered here, instead of excess reactant design often seen in methyl acetate hydrolysis. Because the light product (the LK C) and heavy product (the HHK D) are withdrawn from top and bottoms of the column, the reactive zone is placed in the middle. Figure 16 gives the column configuration. Following the proposed design procedure, the final design is shown in Table 3 with detailed parameter values.

Initially, it is thought that this is simply the mirror image of type III_p. However, this flowsheet has a TAC of \$726,000 which is more than two times of that of type III_p. The RD column has a total of 96 trays with 57 reactive trays, 4 stripping trays and 35 rectifying trays. Two feeds are introduced into the top and bottoms of the reactive zone as shown in Figure 16. Again, the reflux ratio and boilup ratios are much higher than that of type III_p with values greater than 6. Actually, this is a capital intensive RD column with relatively high energy consumption. Liquid phase reactions with one reactant being the LLK (reactant A) pose a difficult design, especially for RD. The reasons are (1) we have to consume all the LLK (reactant A) toward the top of the column and (2) we have to maintain a high concentration for the heavy reactant (the HK B) to ensure the forward reaction is dominant. So, 57 reactive trays are used to react away most of the LLK (reactant A) as clearly shown in Figure 17A where we have very small amount of conversion between tray 30 and tray 61. Leaving the reactive zone toward the top of the column, we have almost equal molar of the LK (product C) and HK (reactant B) with trace amount of the LLK (reactant A). A large number of rectifying trays (35 trays) are employed to return the HK back to the reactive zone while having the LLK and LK as the top product. The scenario toward the bottoms is much simpler, because we are performing separation between the HK (reactant B) and HHK (product C). So, only 4 stripping trays are required. The composition characteristic (Figure 17A) profile leads to a very interesting temperature profile (Figure 17 B) with two distinct plateaus.

Results and Discussion

For the reversible reaction with A + B ⇔ C + D, we have explored all possible relative volatility rankings to the design of RD column. Six distinct configuration is further classified into 3 different types (type I: one-zone, type II: two-zone, and type III: alternating) according to relative position of the reactants and the products in the relative volatility sequence (Figure 1). The subscripts p and r are used to denote the case when the product (p; type I_p, type II_p, and type III_p) or the reactant (r; type I_r, type II_r, and type III_r) is the lightest component. Following a systematic design procedure, process flowsheets are developed and corresponding TACs (operating cost plus discounted capital cost) are computed. The TAC ranges from \$254,000 to \$1,896,000, a factor of 7.5, the flowsheet can be of one-column or two-column scheme, the number of trays in the RD column varies from 11 to 96, the energy cost in the RD changes from \$131,000 to \$1,055,000, a factor of 8, and the reactive zone can be placed n the *middle*, on the *upper* section, on the *lower* section, at *two-end*. All these differences come from shuffling the relative volatility of the reactants and prod-

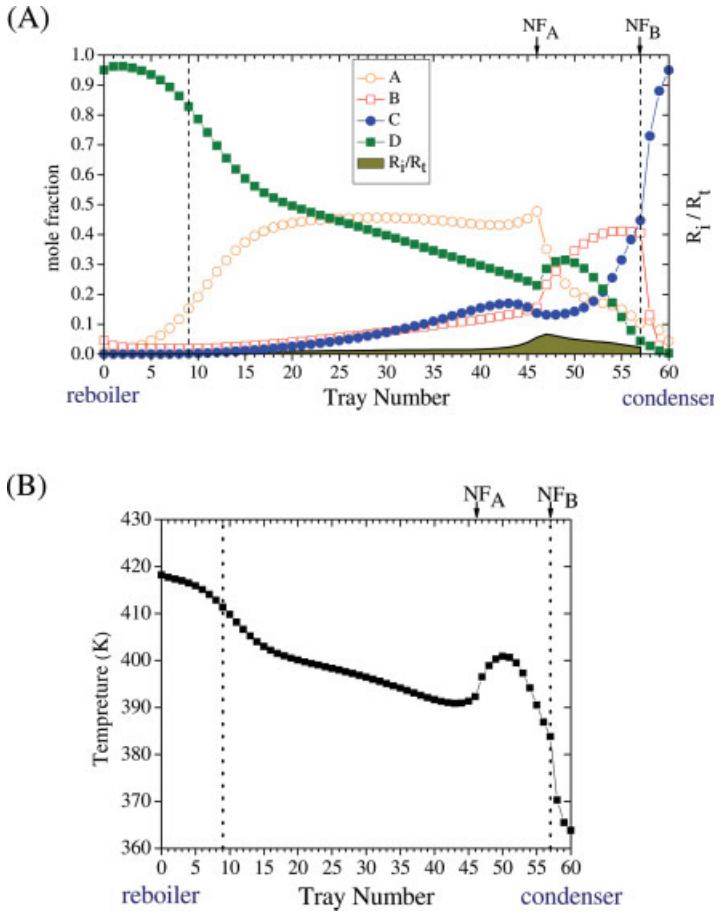

Figure 15. (A) Composition profile, feed locations, and fraction of total conversion (R_i/R_t) and (B) temperature profile for type III_p process (LK + HHK ⇔ LLK + HK).

[Color figure can be viewed in the online issue, which is available at www.interscience.wiley.com.]

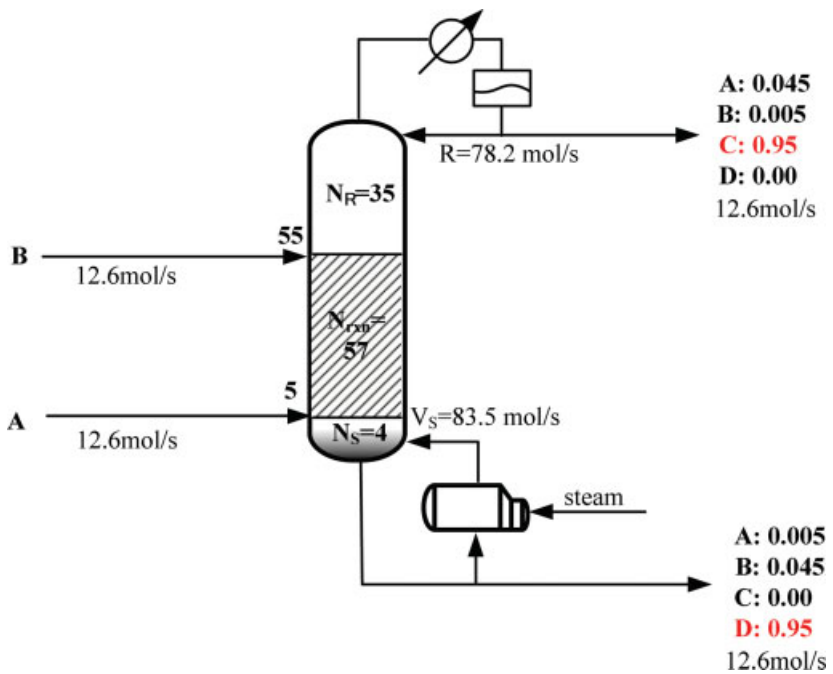

Figure 16. Final design for process type III_r (LLK + HK ⇔ LK + HHK).

[Color figure can be viewed in the online issue, which is available at www.interscience.wiley.com.]

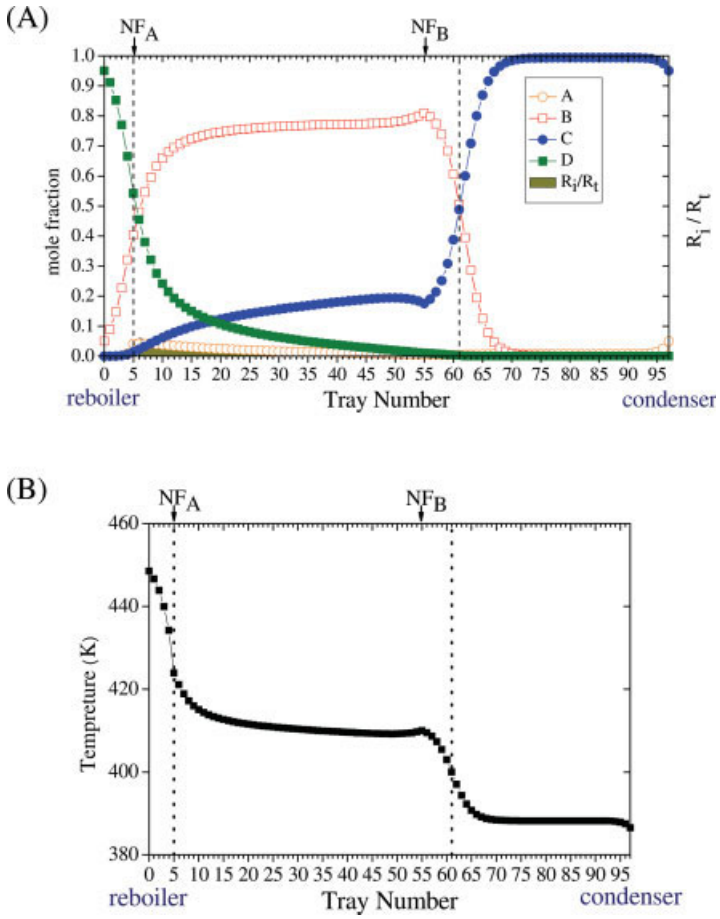

Figure 17. (A) Composition profile, feed locations, and fraction of total conversion (R_i/R_t) and (B) temperature profile for process type III_r (LLK + HK ⇔ LK + HHK).

[Color figure can be viewed in the online issue, which is available at www.interscience.wiley.com.]

ucts between 8, 4, 2, and 1. It looks as if the outcomes are case-based. However, when carefully examine the TAC and the process type, some observations can be made. Figure 18 ranks the TACs for corresponding process flowsheets. In terms of relative volatility sequence, we have the following order for the reaction A + B ⇔ C + D.

$$\begin{array}{ll} \text{Lowest TAC} & \alpha_C > \alpha_A > \alpha_B > \alpha_D \\ & \alpha_C > \alpha_A > \alpha_D > \alpha_B \\ \downarrow & \alpha_C > \alpha_D > \alpha_A > \alpha_B \\ & \alpha_A > \alpha_C > \alpha_B > \alpha_D \\ & \alpha_A > \alpha_B > \alpha_C > \alpha_D \\ \text{Highest TAC} & \alpha_A > \alpha_C > \alpha_D > \alpha_B \end{array} \quad (20)$$

The TAC ranking clearly indicates that the group (the three in the lower part) with higher TACs has one of the reactants (A) being the lightest component. This leads to the following heuristic.

Heuristic H1. It is not favorable to have one of the *reactants* as the *lightest* component. The explanation is quite straightforward: *light* component implies *low* reaction temperature. Certainly, one would prefer the reaction takes place at high temperature zone, instead of the lower one.

Even in the same group (lower 3 or upper three in Eq. 20), one can observe that when the relative volatility between two products are further apart, the TAC will be lower. So, the next heuristic addresses the relative volatilities of products.

Heuristic H2. Prefer the case when the *relative volatility between two products is large* (preferably separated by reactants). The reason is that it facilitates the separation for the products.

If everything being equal (from Heuristics H1 and H2), the relative volatility between reactants is also a useful measure.

Heuristic H3. Prefer the case when the *relative volatility between two reactants is small* (preferably not separated by products). The explanation is that one can have higher reactant concentrations that are favorable for the forward reaction.

The three heuristics presented here are somewhat straightforward and can be combined into one: "prefer the case that reactants are intermediate with a small difference of relative volatility and products are the most and the least volatile with a large difference of relative volatility." The flowsheet with the lowest TAC (type I_p) is favored by all three heuristic (reactant not the lightest one, relative volatility between two products is the largest, and relative volatility between two products is the smallest), while the flowsheet with the highest TAC (type I_r) is a difficult RD as suggested by the heuristics (reactant being the lightest one, relative volatility between two products is the smallest, and relative volatility between two products is the largest).

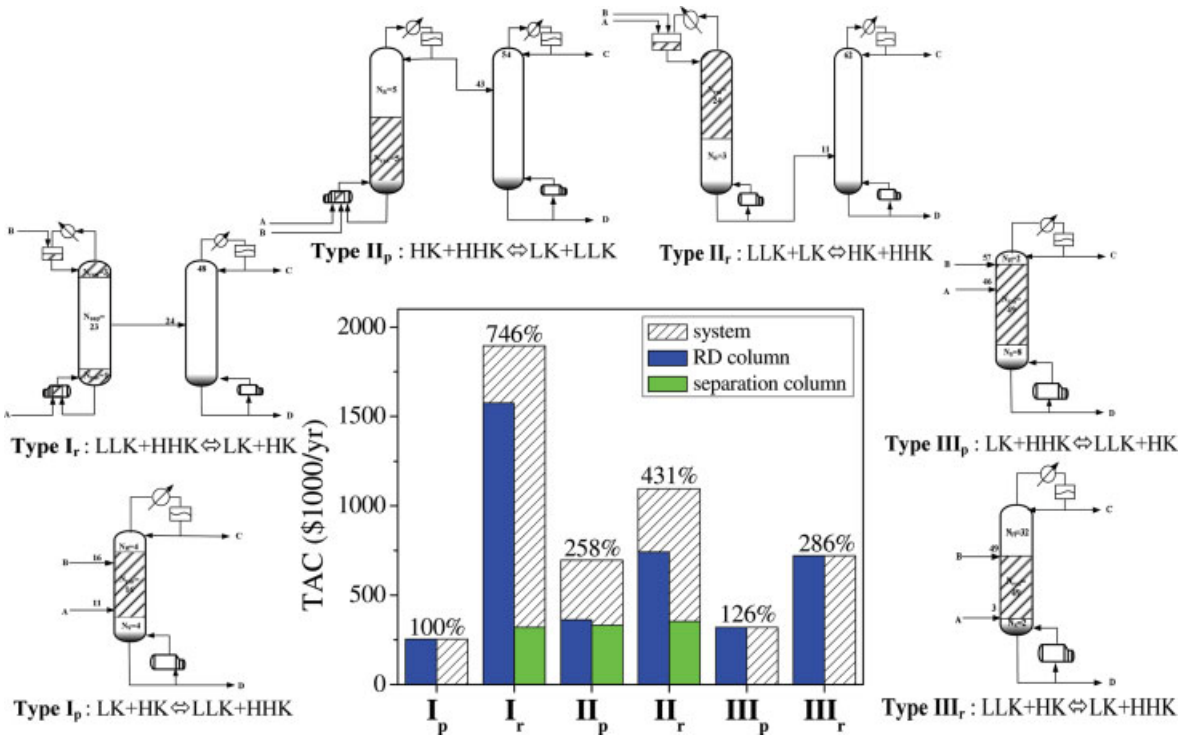

Figure 18. TAC and corresponding column costs for all 6 process flowsheets.

[Color figure can be viewed in the online issue, which is available at www.interscience.wiley.com.]

Before leaving this section, we would like to comment on the scenario where the forward reaction A + B ⇔ C + D, obtaining products C and D, and backward reaction C + D ⇔ A + B, converting back to A and B, are performed sequentially. This scenario occurs for the following two reasons: (1) converting products back to reactants for the sustainability (close the material recycle loop) in pilot-scale experiment for a particular RD experiment (e.g., esterification), and (2) using two RD columns to perform separation and an example is the recovery of polyol from aqueous solution via acetalization.[29] Figure 18 clearly shows that for the above mentioned forward and backward reactions, different RD configuration should be used. For example, if the forward reaction (to from C and D) belongs to type I_p, the type I_r configuration should be used to convert C and D back to A and B. For types type I and II, the placement of the reactive zones are quite different (Figure 18) and, generally, we need two RD columns to achieve the objective. The type III configuration, on the other hand, possibility exists for using the same RD column to perform reaction/separation in the same equipment. Tung[30] explores the costs and configurations for the same reactions with forward and backward paths.

Conclusion

In this article, the effects of relative volatilities rankings to the design of RD are explored, and ideal RD systems are used to illustrate the process flowsheet generation as the ranking varies. For a quaternary system with second-order reversible reaction (A + B = C + D), 24 all possible relative volatility rankings are classified into three process types based on the distribution of reactants and products in the relative volatility sequence (type I: one-zone, type II: two-zone, and type III: alternating). Each type is further denoted by subscript p or r according to the nature (product or reactant) the lightest component. A systematic design procedure is used to generate process flowsheet as the relative volatility ranking changes and the TAC is used to evaluate appropriateness of different designs. The assumptions made in this work include: (1) ideal VLE, (2) equal molar feed (neat process), (3) reactive holdup set by column diameter, and (4) sequential approach for optimization. It is interesting to note that the reactive zone can be placed at the upper section, lower section, middle, or opposite-end of the RD column, depending on the sequences of relative volatilities. The principle actually is quite simple: place the reactive zone to where the reactants are most abundant and introduce the feeds to facilitate the reaction (considering the composition effect). Furthermore, for all six possible flowsheets, the flowsheet can be of one-column or two-column scheme, the TAC varies by a factor of 7.5, the energy cost in the RD changes by a factor of 8, and the number of trays in the RD column ranges from 11 to 96. Physical explanations for the easiness of combined reaction/separation are given and, finally, heuristics are given to evaluate potential difficulty in the RD design. A final word is that we consider only the "neat" design here, for some of the difficult RD flowsheets, "excess reactant" design might be an attractive alternative.

Acknowledgments

We thank D. Kaymak and W. L. Luyben for providing MATLAB program for reactive distillation process simulation using relaxation. This

work was supported by the Ministry of Economic Affairs under grant 94-EC-17-A-09-S1-019.

Notation

a_B = preexponential factor for the reverse reaction (kmol s^{-1} $kmol^{-1}$)
a_F = preexponential factor for the forward reaction (kmol s^{-1} $kmol^{-1}$)
A = light reactant
$A_{VP,i}$ = Antonie vapor pressure coefficient
B = heavy reactant
B = bottoms flow rate (kmol/s)
$B_{VP,i}$ = Antonie vapor pressure coefficient
C = light product
D = heavy product
D = distillate flow rate (kmol/s)
E_B = activation energy of the reverse reaction (cal/mol)
E_F = activation energy of the forward reaction (cal/mol)
F_{OA} = fresh feed flow rate of light reactant A (kmol/s)
F_{OB} = fresh feed flow rate of heavy reactant B (kmol/s)
HHK = heavier than heavy key
HK = heavy key
k_{Bj} = specific reaction rate of the reverse reaction in tray j (kmol s^{-1} $kmol^{-1}$)
k_{Fj} = specific reaction rate of the forward reaction in tray j (kmol s^{-1} $kmol^{-1}$)
K_{EQ} = chemical equilibrium constant
L_j = liquid flow rate from tray j (kmol/s)
LLK = lighter than light key
LK = light key
M_j = liquid holdup on tray j (kmol)
NF_{heavy} = number of fresh heavy reactant feed tray
NF_{light} = number of fresh light reactant feed tray
N_R = number of rectifying trays
N_{rxn} = number of reactive trays
N_S = number of stripping trays
P = total pressure (bar)
P_i^s = vapor pressure of component i (bar)
R = reflux flow rate (kmol/s)
R = perfect gas law constant (cal mol^{-1} K^{-1})
$R_{j,i}$ = reaction rate of component i on tray j (kmol/s)
R_t = total conversion
T_j = temperature in tray j (K)
V_j = vapor flow rate from tray j (kmol/s)
$x_{B,i}$ = bottoms composition of component i (mole fraction)
$x_{D,i}$ = distillate composition of component i (mole fraction)
$x_{j,i}$ = jth tray composition of component i (mole fraction)
$x_{S,i}$ = sidedraw composition of component i (mole fraction)
$y_{B,i}$ = composition of component i in vapor of bottoms (mole fraction)
$y_{D,i}$ = composition of component i in vapor of distillate (mole fraction)
$y_{j,i}$ = composition of component i in vapor on tray j (mole fraction)

Greek letters

α_i = relative volatility of component i
β = liquid hydraulic time constant (s)
v_i = stoichiometric coefficient of the ith component
ΔH_v = heat of vaporization (cal/mol)
λ = heat of reaction (cal/mol)

Literature Cited

1. Doherty MF, Malone MF. *Conceptual Design of Distillation Systems*. New York: McGraw-Hill, 2001.
2. Sundmacher K, Kienle A. *Reactive Distillation*. Weinheim: Wiley-VCH, 2003.
3. Malone MF, Huss RS, Doherty MF. Green chemical engineering aspects of reactive distillation. *Environ Sci Technol*. 2003;37:5325–5329.
4. Doherty MF, Buzad G. Reactive distillation by design. *Trans Inst Chem Eng Part A*. 1992;70:448–458.
5. Taylor R, Krishna R. Modelling reactive distillation. *Chem Eng Sci*. 2000;55:5183–5229.
6. Al-Arfaj MA, Luyben WL. Effect of number of fractionating trays on reactive distillation performance. *AIChE J*. 2000;46:2417–2425.
7. Bessling B, Schembecker G, Simmrock KH. Design of processes with reactive distillation line diagrams. *Ind Eng Chem Res*. 1997;36:3032–3042.
8. Lee JW. Feasibility studies on quaternary reactive distillation systems. *Ind Eng Chem Res*. 2002;41:4632–4642.
9. Groemping M, Dragomir RM, Jobson M. Conceptual design of reactive distillation columns using stage composition lines. *Chem Eng Proc*. 2004;43:369–382.
10. Dragomir RM, Jobson M. Conceptual design of single-feed kinetically controlled reactive distillation columns. *Chem Eng Sci*. 2005;60:5049–5068.
11. Hoffmaster WR, Hauan S. Using feasible regions to design and optimize reactive distillation columns with ideal VLE. *AIChE J*. 2006;52:1744–1753.
12. Kaymak DB, Luyben WL. A quantitative comparison of reactive distillation with conventional multi-unit reactor/column/recycle systems for different chemical equilibrium constants. *Ind Eng Chem Res*. 2004;43:2493–2507.
13. Kaymak DB, Luyben WL, Smith IV OJ. Effect of relative volatility on the quantitative comparison of reactive distillation and conventional multi-unit systems. *Ind Eng Chem Res*. 2004;43:3151–3162.
14. Luyben WL. Economic and dynamic impact of the use of excess reactant in reactive distillation systems. *Ind Eng Chem Res*. 2000;39:2935–2946.
15. Lee JW, Bruggemann S, Marquardt W. Shortcut method for kinetically controlled reactive distillation systems. *AIChE J*. 2003;49:1471–1487.
16. Cheng YC, Yu CC. Effects of feed tray locations to the design of reactive distillation and its implication to control. *Chem Eng Sci*. 2005;60:4661–4677.
17. Huang K, Iwakabe K, Nakaiwa M, Tsutsumi A. Towards further internal heat integration in design of reactive distillation columns—Part I: The design principle. *Chem Eng Sci*. 2005;60:4901–4914.
18. Agreda VH, Partin LR, Heise WH. High-purity methyl acetate production via reactive distillation. *Chem Eng Prog*. 1990;86:40–46.
19. Tang YT, Hung SB, Chen YW, Huang HP, Lee MJ, Yu CC. Design of reactive distillations for acetic acid esterification with different alcohols. *AIChE J*. 2005;51:1683–1699.
20. Chiang SF, Kuo CL, Yu CC, Wong DSH. Design alternatives for amyl acetate process: coupled reactor/column and reactive distillation. *Ind Eng Chem Res*. 2002;41:3233–3246.
21. Chin J, Lee JW, Choe J. Feasible products in complex batch reactive distillation. *AIChE J*. 2006;52:1790–1805.
22. Schembecker G, Tlatlik S. Process synthesis for reactive separations. *Chem Eng Process*. 2003;42:179–189.
23. Chen F, Huss RS, Malone MF, Doherty MF. Simulation of kinetic effects in reactive distillation. *Comput Chem Eng*. 2000;24:2457–2473.
24. Chen F, Huss RS, Malone MF, Doherty MF. Multiple steady states in reactive distillation: kinetic effects. *Comput Chem Eng*. 2002;26:81–93.
25. Luyben WL. Use of dynamic simulation to converge complex process flowsheets. *Chem Eng Educat*. 2004;142–149.
26. Fukuoka S, Watanabe T, Dozono T. Methods for producing a crystallized aromatic carbonate and a crystallized aromatic polycarbonate obtained thereby. U.S. Patent 4,948,871 (1990).
27. Choi JI, Hong WH. Recovery of lactic acid by batch distillation with chemical reactions using ion exchange resin. *J Chem Eng Jpn*. 1999;32:184–189.
28. Chopade SP, Sharma MM. Reaction of ethanol and formaldehyde: use of versatile cation-exchange resins as catalyst in batch reactors and reactive distillation columns. *Reactive Funct Polym*. 1997;32:53–64.
29. Dhalea AD, Myranta LK, Chopadea SP, Jacksonb JE, Miller DJ. Propylene glycol and ethylene glycol recovery from aqueous solution via reactive distillation. *Chem Eng Sci*. 2004;59:2881–2890.
30. Tung ST. *Effects of Relative Volatility Rankings to the Design of Reactive Distillation Systems*. Master thesis, National Taiwan University, Taipei, 2006.

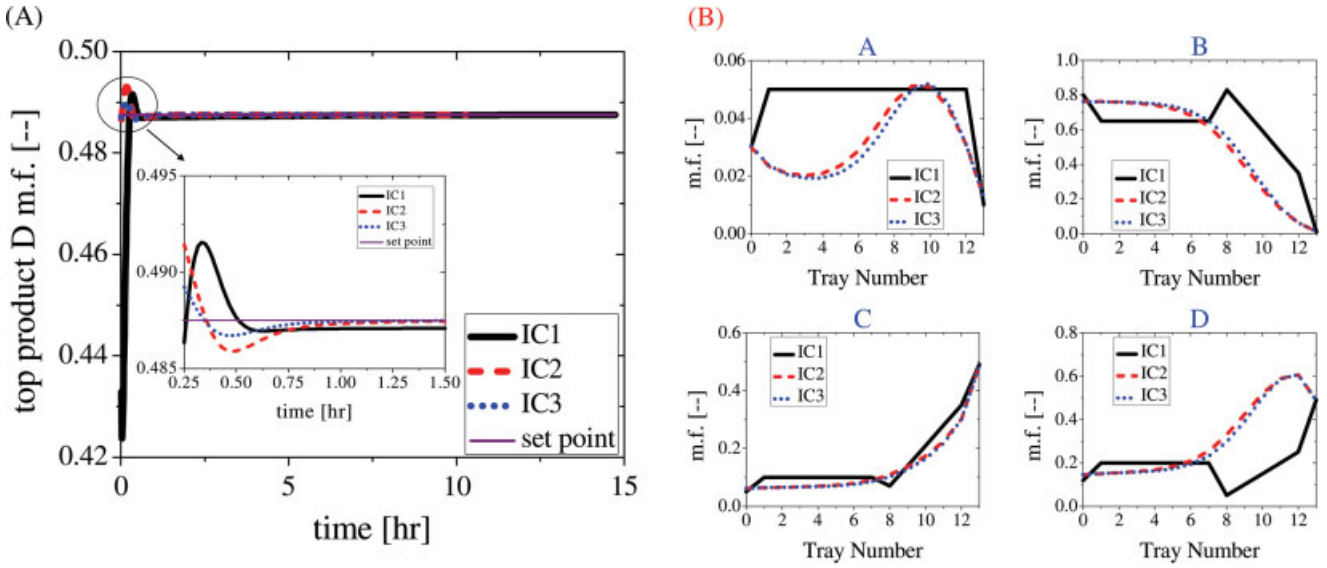

Figure A1. Convergences of type II_p process (A) for different initial conditions (B).

[Color figure can be viewed in the online issue, which is available at www.interscience.wiley.com.]

Appendix A: Effects of Initial Conditions to Convergence

The relaxation approach (control approach) to simulation is generally robust for most RD configurations (type I_p, type II_p and II_r, type III_p and III_r), except for the most difficult case (type I_r). Let us use another example, Type II_p process, to illustrate this. For 3 different initial conditions (IC1-IC3), they took 8–15 h (process time; (IC1: ~8 h, IC2: ~10 h, and IC3: ~15 h) to converge as shown in Figure A1. However, for type I_r process, a modest amount of deviation in the initial condition may lead to divergence as shown in Figure A2.

Appendix B: Design for Different Process Configurations

Design of Type I_r

Design variables for the RD for the type I_r configuration include: number of reactive trays on the top and bottoms reactive zones ($N_{rxn,top}$ and $N_{rxn,bot}$), number of separation trays (N_{sep}), and side-draw location. Three lines in Figure B1(A) indicate that the minimum TACs correspond to the same total number of trays. However, an optimal number of reactive trays exists and this gives: $N_{rxn,top} = 3$, $N_{rxn,bot} = 1$, and $N_{sep} = 26$. The tradeoff comes from the crossing

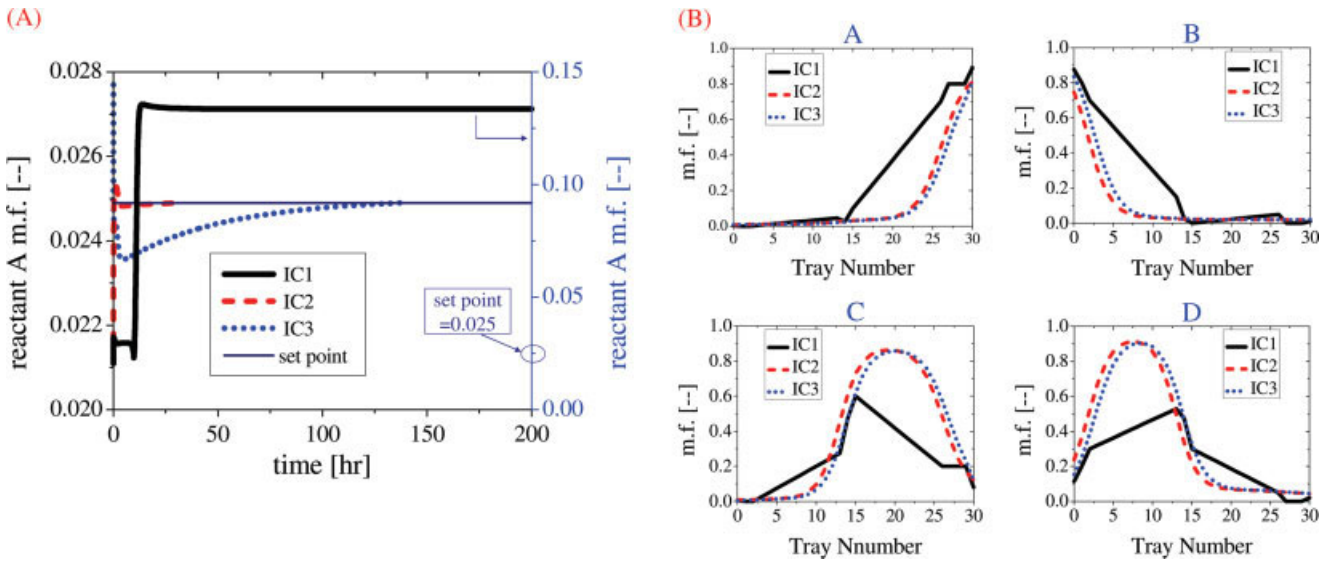

Figure A2. Convergences of type I_r process (A) for different initial conditions (B).

[Color figure can be viewed in the online issue, which is available at www.interscience.wiley.com.]

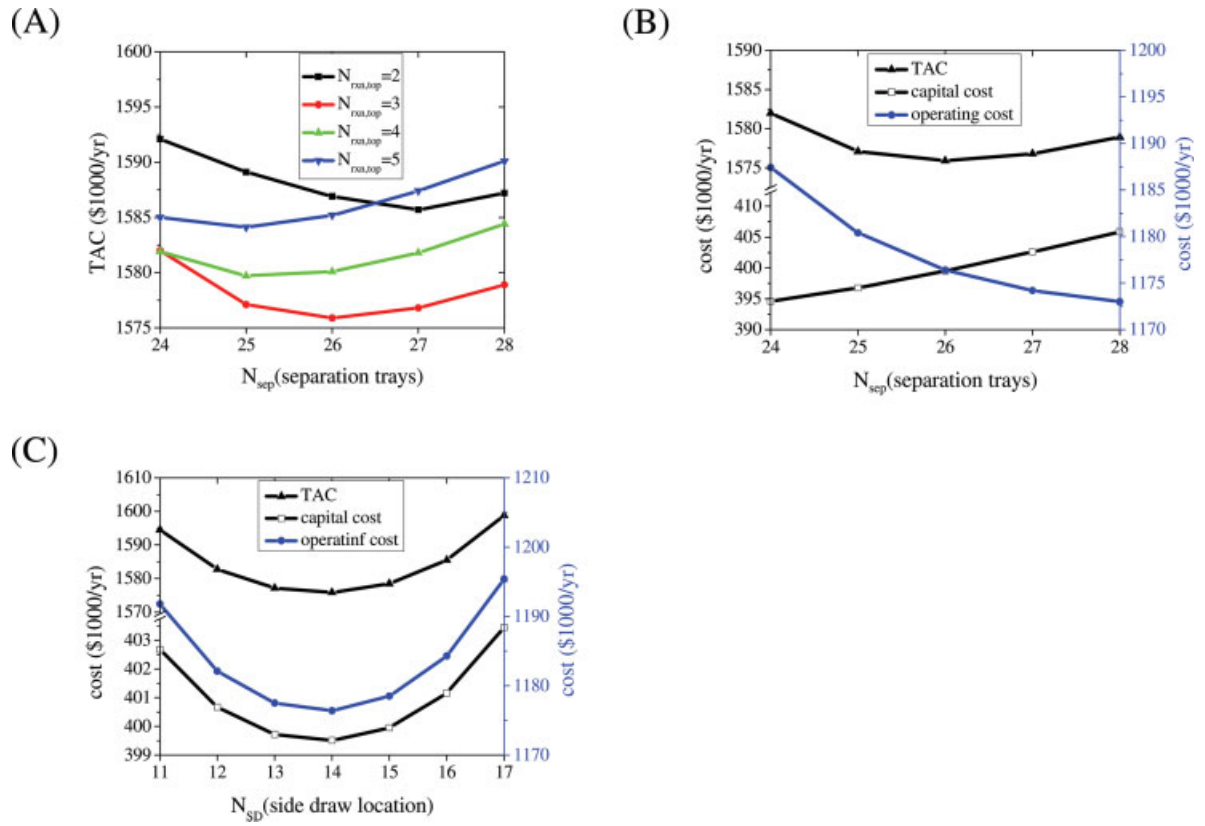

Figure B1. Relationship between TAC and design variables for type I_r process: (A) number of separation trays (N_{sep}) versus TAC for different $N_{rxn,bot}$ with $N_{rxn,bot}$ = 1, (B) tradeoff of separation trays (N_{sep}) with $N_{rxn,bot}$ = 1 and $N_{rxn,top}$ = 3, and (C) side-draw location (N_{SD}) with $N_{rxn,bot}$ = 1 and $N_{rxn,top}$ = 3 and N_{sep} = 26.

[Color figure can be viewed in the online issue, which is available at www.interscience.wiley.com.]

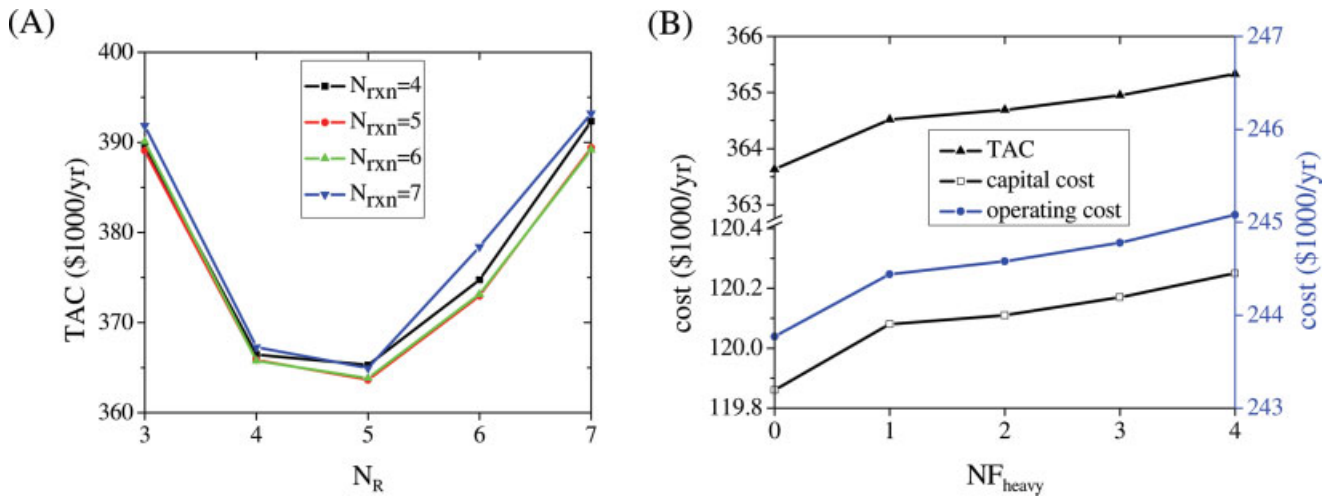

Figure B2. Relationship between TAC and design variables for type IIp process: (A) number of rectifying trays (N_R) versus TAC for different N_{rxn} and (B) feed tray locations (NF_{heavy}) with N_{rxn} = 5 and N_R = 5.

[Color figure can be viewed in the online issue, which is available at www.interscience.wiley.com.]

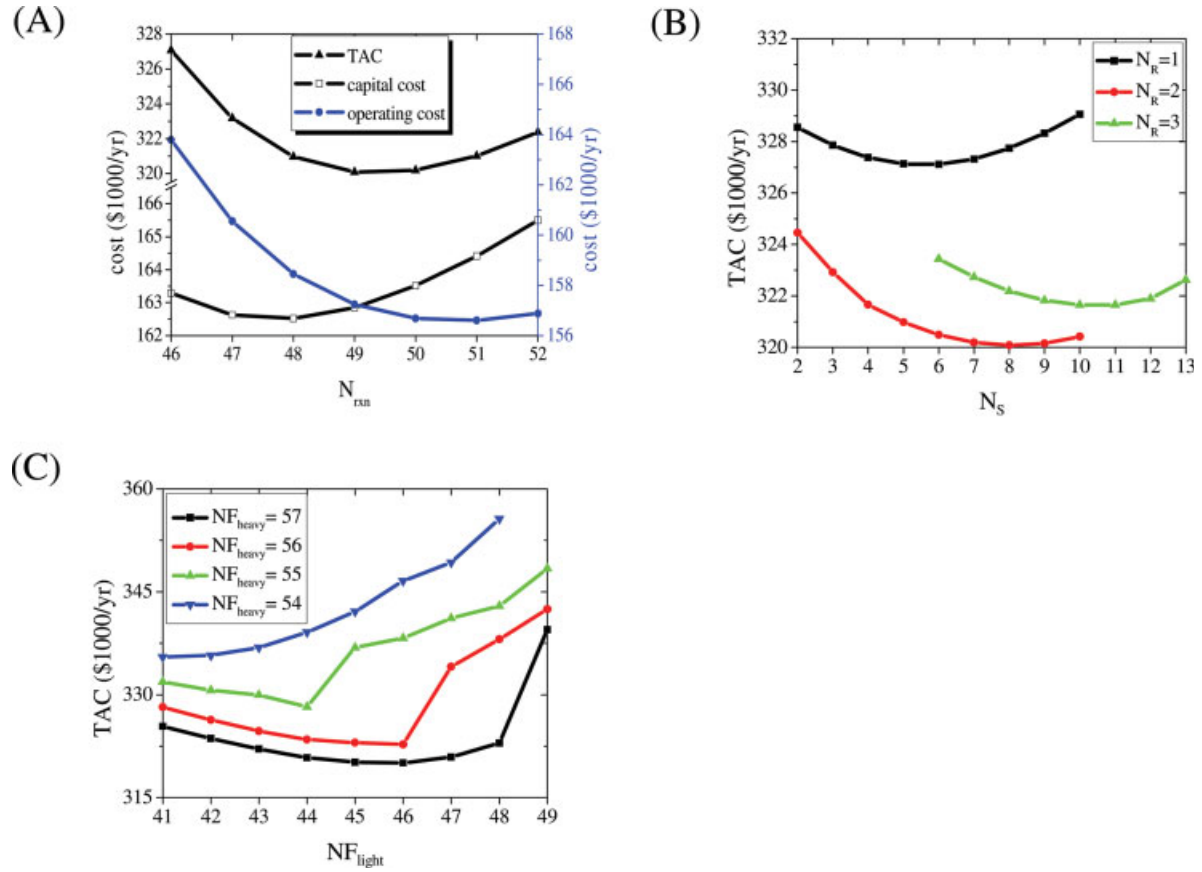

Figure B3. Relationship between TAC and design variables for type III_p process: (A) number of reactive trays (N_{rxn}) vs. TAC with $N_R = 2$ and $N_S = 8$, (B) number of stripping and rectifying trays (N_S and N_R) with $N_{rxn} = 49$, and (C) feed tray locations (NF_{light}) with $N_{rxn} = 49$ and $N_R = 2$ and $N_S = 8$ for different NF_{heavy}.

[Color figure can be viewed in the online issue, which is available at www.interscience.wiley.com.]

between the operating and capital costs as shown in Figure B1(B). The side-draw location is also found by minimizing the TAC (Figure B1(C)).

Design of Type II_p

Design variables for the RD for the type II_p configuration include: number of reactive trays (N_{rxn}), number of trays in the rectifying section (N_R), and feed tray location of the HHK (NF_{heavy}). The results, Figure B2(A), show that, as compared to N_{rxn}, the number of trays in the rectifying section, N_R, is a more sensitive design variable. The reason is that, as one increases N_R, the operating goes down initially followed by an increase while the capital cost exhibits a steady increasing trend. Figure B2(B) indicates that the heavier reactant (HHK) should also be introduced into the reboiler, same as the lighter reactant (HK). Recall that the two reactants are HK and HHKL, respectively (the reaction is HK + HHK = LLK + LK).

Design of Type III_p

Design variables for the RD for the type III_p configuration include: number of reactive trays (N_{rxn}), number of trays in the rectifying (N_R) and stripping section (N_S), and feed tray locations of both the light and heavy reactants (NF_{light} and NF_{heavy}). Figures B3(A, B) show that, as compared to N_{rxn} and N_S, the number of trays in the rectifying section, N_R, is a more sensitive design variable. The tradeoff comes from the crossing of the operating and capital costs Figure B3(C) indicates that the heavier reactant (HHK) should also be introduced to the top of the reactive zone and light reactant is fed to the column 12 trays below. Again, the feed tray locations are important design variables.

Manuscript received July 3, 2005, revision received Dec. 1, 2006, and final revision received Feb. 23, 2007.